Research Article

MOLECULAR PAIN

Molecular Pain
Volume 12: 1–21
© The Author(s) 2016
Reprints and permissions:
sagepub.co.uk/journalsPermissions.nav
DOI: 10.1177/1744806916643724
mpx.sagepub.com

SAGE

Critical evaluation of the expression of gastrin-releasing peptide in dorsal root ganglia and spinal cord

Devin M Barry, PhD[1,2], Hui Li, PhD[1,3], Xian-Yu Liu, PhD[1,2], Kai-Feng Shen, PhD[1,4], Xue-Ting Liu, PhD[1,5], Zhen-Yu Wu[3], Admire Munanairi, PhD[1,2], Xiao-Jun Chen[6], Jun Yin[1,2], Yan-Gang Sun, PhD[6], Yun-Qing Li, PhD[3] and Zhou-Feng Chen, PhD[1,2,7,8]

Abstract

There are substantial disagreements about the expression of gastrin-releasing peptide (GRP) in sensory neurons and whether GRP antibody cross-reacts with substance P (SP). These concerns necessitate a critical revaluation of GRP expression using additional approaches. Here, we show that a widely used GRP antibody specifically recognizes GRP but not SP. In the spinal cord of mice lacking SP (*Tac1* KO), the expression of not only GRP but also other peptides, notably neuropeptide Y (NPY), is significantly diminished. We detected *Grp* mRNA in dorsal root ganglias using reverse transcription polymerase chain reaction, in situ hybridization and RNA-seq. We demonstrated that *Grp* mRNA and protein are upregulated in dorsal root ganglias, but not in the spinal cord, of mice with chronic itch. Few GRP^+ immunostaining signals were detected in spinal sections following dorsal rhizotomy and GRP^+ cell bodies were not detected in dissociated dorsal horn neurons. Ultrastructural analysis further shows that substantially more GRPergic fibers form synaptic contacts with gastrin releasing peptide receptor-positive ($GRPR^+$) neurons than SPergic fibers. Our comprehensive study demonstrates that a majority of GRPergic fibers are of primary afferent origin. A number of factors such as low copy number of *Grp* transcripts, small percentage of cells expressing *Grp*, and the use of an eGFP GENSAT transgenic as a surrogate for GRP protein have contributed to the controversy. Optimization of experimental procedures facilitates the specific detection of GRP expression in dorsal root ganglia neurons.

Keywords

substance P, gastrin-releasing peptide, itch, dorsal root ganglia, sensory neurons, spinal cord

Date received: 20 January 2016; revised: 15 February 2016; accepted: 18 February 2016

[1]Center for the Study of Itch, Washington University School of Medicine, St. Louis, MO, USA
[2]Departments of Anesthesiology, Washington University School of Medicine, St. Louis, MO, USA
[3]Department of Anatomy, K. K. Leung Brain Research Centre, The Fourth Military Medical University, Xi'an, PR China
[4]Department of Neurosurgery, Xinqiao Hospital, Third Military Medical University, Chongqing, PR China
[5]Guangdong Provincial Key Laboratory of Allergy & Clinical Immunology, The State Key Laboratory of Respiratory Disease, The Second Affiliated Hospital, Guangzhou Medical University, Guangdong, PR China
[6]Institute of Neuroscience, State Key Laboratory of Neuroscience, CAS Center for Excellence in Brain Science and Intelligence Technology, Shanghai Institutes for Biological Sciences, Chinese Academy of Sciences, Shanghai, China
[7]Departments of Psychiatry, Center for the Study of Itch, Washington University School of Medicine, St. Louis, MO, USA
[8]Departments of Developmental Biology, Center for the Study of Itch, Washington University School of Medicine, St. Louis, MO, USA

Corresponding author:
Zhou-Feng Chen, Washington University School of Medicine, St. Louis, MO, USA.
Email: chenz@wustl.edu
Yun-Qing Li, Department of Anatomy & K. K. Leung Brain Research Centre, The Fourth Military Medical University, Xi'an, PR China.
Email: deptanat@fmmu.edu.cn

Creative Commons Non Commercial CC-BY-NC: This article is distributed under the terms of the Creative Commons Attribution-NonCommercial 3.0 License (http://www.creativecommons.org/licenses/by-nc/3.0/) which permits non-commercial use, reproduction and distribution of the work without further permission provided the original work is attributed as specified on the SAGE and Open Access pages (https://us.sagepub.com/en-us/nam/open-access-at-sage).

Introduction

Many earlier studies have demonstrated the specificity of gastrin-releasing peptide (GRP) antibodies by radioimmunoassay and immunohistochemistry (IHC) after dorsal rhizotomy or antibody absorption, and have concluded that GRP-positive (GRP^+) fibers, or GRP content in the spinal cord, are predominantly of peripheral origin.[1–5] In addition, it was shown that GRP antibody does not cross-react with substance P (SP), and that GRP is present in dorsal root ganglia (DRGs) of cat, dog, rat, and monkey.[2–7]

After more than a decade of relative dormancy, the identification of GRP as an itch-transmitting peptide in DRGs has reignited considerable interest in GRP expression.[8–12] We propose that GRP is a key itch-specific neuropeptide in sensory neurons that is released from primary afferents to activate postsynaptic GRPR in the spinal cord in response to nonhistaminergic stimuli.[12–16] Consistent with this notion as well as with many earlier studies, several other laboratories have independently shown that the GRP antibody recognizes a distinct subset of DRG neurons mostly using 1:1000 or 1:4000 dilution.[17–20] Moreover, GRP is up-regulated in DRGs of mice and monkeys with chronic itch[12,13,21,22] and a portion of GRP^+ neurons are distinct from SP^+ neurons in DRG.[18,23] More recently, 3-D synaptome analysis using high-voltage electron microscopy and chemical anatomy revealed that the electron-dense GRP^+ vesicles are present in presynaptic afferents contacting postsynaptic neurons with the electron-dense postsynaptic densities in the spinal cord.[24]

On the other hand, conflicting results on GRP expression in DRGs using the GRP antibody have also been reported (Table 1). Most notably, some researchers were unable to detect specific GRP immunostaining in DRGs. The issue was raised about the dilution of the antibody (Immunostar) used in the studies. Solorzano et al.[25] showed that at 1:1000 dilution GRP immunostaining is widespread in DRGs, similar to several previous studies.[26,27] On the other hand, using 1:1000 dilution, Fleming et al.[28] showed only 1.79% of DRGs are positive for GRP, the smallest percentage ever reported. While Solorzano et al.[25] argued that at 1:4000 dilution, GRP antibody is specific but could not detect any staining in DRG, Kiguchi et al.[17] recently showed distinct staining in a small subset of DRGs using the same 1:4000 dilution.

Detection of *Grp* mRNA by in situ hybridization (ISH) in DRGs also remains controversial. Although we were able to observe *Grp* expression in DRGs by ISH,[12,29] others could not detect positive signals.[25,28,30,31] Moreover, two groups did not detect *Grp* mRNA in DRG by RNA-seq.[32,33] While several laboratories detected *Grp* mRNA by reverse transcription polymerase chain reaction (RT-PCR) using single cell method,[26,27] Solorzano et al.[25] argued that the detections are due to de novo expression in DRG neuron culture conditions. On the other hand, it has been reported that *Grp* mRNA was detectable from uncultured DRGs by RT-PCR,[28,30] qRT-PCR[12] and a cDNA microarray study[34] (Table 1).

Two recent studies argued that the widely used GRP antibody cross-reacts with SP[25,33] because GRP immunostaining is reduced in mice lacking *Tac1*.[25] In contrast, others showed specific GRP and SP double immunostaining in DRGs, arguing against this possibility.[18,27]

These discrepancies in the literature prompted us to revisit the issue, with a focus on potential reasons that may explain some of the inconsistent results and newly

Table 1. Previous studies on detection of GRP expression in DRG.

Method	GRP expression	References
IHC/IF (WT)	+ (lab derived)	2, 3, 4
	+ (1:1000); IS	16, 20, 28
	+++ (1:1000); IS	26, 29
	+ (not indicated)	19
	+ (1:500); IS	13, 23
	+++ (1:100); SCBT	27
	+ (1:1000, 1:2000); Assaypro	18
	+++ (1:1000), - (1:4000); IS	25
	+ (1:4000); IS	17
IHC/IF (Grp KO)	− (1:1000); IS	29
	− (1:500); IS	13
	+++ (1:1000), −(1:4000); IS	25
ISH	− (bases 212–634)	28
	− (coding region, bases 115–554)	25
	− (not indicated)	30, 31
	+ (bases 149–707)	12
RT-PCR gel electrophoresis	+ (weak band)	28
	+ (single cell)	26, 27
qRT-PCR	+ (trace amount)	30
	+	12
	+ (low levels)	25
RNA-Seq	–	33
	− (single cell)	32
cDNA Microarray	+	34

− not detected or absent, + detected and/or distinct staining pattern, +++ widespread staining pattern; IHC/IF antibody dilutions are indicated in parentheses; ISH *Grp* mRNA region used for antisense probe indicated in parentheses (NCBI accession NM_175012.4), IS: Immunostar; SCBT: Santa Cruz Biotechnology.

raised concerns. Specifically, we set out to critically evaluate the cross-reactivity of the GRP antibody with SP. Because the majority of studies investigating *Grp* mRNA expression in DRGs were not done in a quantitative and comparative manner, we also examined this issue relative to the expression of other genes using RT-PCR and RNA-seq. Our studies and survey of the related literatures highlight technical caveats that should be considered for the detection of GRP protein and *Grp* mRNA.

Materials and methods

Animals

Male mice between 7 and 12 weeks old were used for experiments. C57BL/6 J mice were purchased from the Jackson Laboratory (http://jaxmice.jax.org/strain/013636.html). C57BL/6 J mice, GRPR-eGFP BAC Transgenic mice from MMRRC (i.d. 036178), *Grp* KO,[13] *Tac1* KO,[35] BRAF$^{NaV1.8}$,[13], and their respective wild type (WT) littermates were used. All mice were housed under a 12 h light/dark cycle with food and water provided ad libitum. All experiments were performed in accordance with the guidelines of the National Institutes of Health and the International Association for the Study of Pain and were approved by the Animal Studies Committee at Washington University School of Medicine.

Ablation of TRPV1$^+$ fibers

C57BL/6 J mice were treated with resiniferatoxin (RTX) (25 ng in 5 µL, intrathecal) as previously described, with a modification in the dose of RTX.[36] Seven days after RTX injection, mice were perfused, and lumbar spinal cord tissues were collected for immunostaining.

Dorsal rhizotomy

C57BL/6 J male mice were used for unilateral rhizotomy at spinal lumbar level L4–L6.[13] Briefly, laminectomy was performed to expose the L4–L6 dorsal roots, which were sharply transected. Animals were perfused, and the lumbar spinal cord tissues were collected 14 days after the dorsal rhizotomy for immunostaining.

Xerosis (dry skin) model

The AEW (acetone-ether-water) dry skin model was implemented as described.[37,38] Briefly, the nape of mice was shaved and a mixture of acetone and diethyl ether (1:1) was applied with a cotton pad on the neck skin for 15 s, followed immediately by a 30 s distilled water application. This regimen was administered twice daily for eight days. Littermate control mice received water only for 45 s on the same schedule. Spontaneous scratches were counted for 60 min on the morning following the last AEW treatment. On day 8, AEW-treated mice displayed 150–300 scratching bouts in 60 min. Cervical and thoracic DRG and spinal cord tissues were isolated and processed for IHC, ISH, and RT-PCR and qRT-PCR.

Immunohistochemistry

Mice were anesthetized (ketamine, 100 mg/kg and Xylazine, 15 mg/kg) and perfused intracardially with PBS pH 7.4 followed by 4% paraformaldehyde (PFA) in PBS. Tissues were dissected, post-fixed for 2–4 h, and cryoprotected in 20% sucrose in PBS overnight at 4°C. Tissues were sectioned in OCT using a cryostat microtome. IHC was performed as described.[14] Briefly, free-floating frozen sections at 20 µm thickness were blocked in a 0.01 M PBS solution containing 2% donkey serum and 0.3% Triton X-100 followed by incubation with primary antibodies overnight at 4°C, washed three times with PBS, secondary antibodies for 2 h at room temperature, and washed again three times. For biotin-conjugated secondary antibodies, sections were next incubated with avidin-conjugated fluorophores and washed three times. Sections were mounted on slides and approximately 100 µL FluoromountG (Southern Biotech) was placed on the slide with a coverslip. Fluorescein isothiocyanate (FITC)-conjugated Isolectin B4 from *Griffonia simplicifolia* (IB4, 10 µg/mL; L2895, Sigma) or the following primary antibodies were used, rabbit anti-GRP (1:500–1:4000; Immunostar, 20073, lot #1420001), rabbit anti-calcitonin gene-related peptide alpha (CGRPα) (1:5000; Millipore, AB15360), guinea pig anti-CGRPα (1:1000; Peninsula Labs, T-5027), guinea pig anti-SP (1:1000; Abcam, ab10353, lot# GR29977-17), guinea pig anti-transient receptor potential cation channel subfamily V member 1 (TRPV1) (1:1000; Neuromics, GP14100), and chicken anti-GFP antibody (1:500; Aves Labs, GFP-1020). For GRPR/GRP/SP triple staining, a total of 10 adult GRPR-eGFP male mice and chicken anti-GFP antibody (1:500; Aves Labs) were used. The secondary antibodies were FITC-, Cyanine 3 (Cy3)-, Cy5 donkey anti-guinea pig (1:500; Millipore) or Alexa 594 conjugated donkey anti-rabbit or anti-guinea pig IgG (1:500, Jackson ImmunoResearch), or biotin-SP-conjugated donkey anti-rabbit or anti-chicken IgG (1:400, Jackson ImmunoResearch) and Neutravidin-conjugated Alexa Fluor488 (1:1000, Life Technologies), Third antibody—FITC-avidin (1:1000; Vectorlabs). Fluorescent Images were taken using a Nikon Eclipse Ti-U microscope with CoolSnapHQ CCD Camera (Photometrics). Staining intensities for each section were quantified by an observer blinded to the group or

genotype using ImageJ (version 1.34e, NIH Image) as previously described.[13]

DRG and spinal dorsal horn neuron cultures

Primary cultures of DRGs and spinal dorsal horn neurons were prepared from seven-weeks-old C57BL/6 J mice.[13] Mice were sacrificed, DRGs and dorsal horn of spinal cord were dissected out and incubated, separately, in Neurobasal-A Medium (Gibco) containing 30 µl papain (Worthington) at 37°C for 20 min, and an additional 20 min digestion at 37°C for DRGs with collagenase type 2 (Worthington). Enzymatic digestion was stopped by adding another 2 mL Neurobasal-A medium. After washing with the same medium for three times, gentle trituration was performed using flame polished glass pipette until the solution became cloudy. The homogenate was centrifuged at 500 × g for 5 min, and the supernatant was discarded. Cell pellets were resuspended in culture medium composed of Neurobasal medium (Gibco, 92% vol/vol), fetal bovine serum (Invitrogen, 2% vol/vol), HI Horse Serum (Invitrogen, 2% vol/vol), GlutaMax (2 mM, Invitrogen, 1% vol/vol), B27 (Invitrogen, 2% vol/vol), Penicillin (100 µg/ml) and Streptomycin (100 µg/ml) and then plated onto 12-mm coverslips coated with laminin and poly-ornithine for 1 h.

GRP immunostaining on dissociated DRG neurons and dorsal horn neurons was performed as previously described.[39] Cells were fixed in 4% paraformaldehyde for 1 h at room temperature and blocked in blocking buffer (PBS containing 2% normal donkey serum and 0.3% Triton X-100) for 1 h at room temperature. Cells were then incubated with rabbit anti-GRP antibody (ImmunoStar, 1:1,000) and mouse anti-NeuN antibody (EMD Millipore, 1:1,000) in blocking buffer overnight at 4°C. After washing, cells were incubated with Cy3-conjugated donkey anti-rabbit secondary antibody (1:1000) and FITC-conjugated donkey anti-mouse secondary antibody (1:1000) for 1 h at room temperature.

Immuno-electron microscopy

Immuno-electron microscopic studies were performed as previously described.[40] Briefly, for GRPR/GRP or GRPR/SP double staining, cross sections of lumbar spinal cord of adult GRPR-eGFP mice were double immune-labeled by guinea pig anti-SP antibody (1:2000; Incstar) or rabbit anti-GRP antibody (1:1000; Immunostar) and chicken anti-GFP antibody (1:500; Aves Labs) using immunogold–silver method and immunoperoxidase method, respectively. For GRP/SP double staining, cross sections of lumbar spinal cord of adult C57BL/6 J mice were double immuno-labeled by guinea pig anti-SP antibody (1:2000; Incstar) and rabbit anti-GRP antibody (1:1000; Immunostar) using immunogold–silver method and immunoperoxidase method, respectively. Furthermore, 50-nm-thick ultrathin sections were cut and examined with a JEM-1400 electron microscope (JEM, Tokyo, Japan). The digital micrographs were captured by VELETA (Olympus,Tokyo, Japan).

In situ hybridization

ISH was performed as previously described,[41] using a digoxigenin-labeled cRNA (Roche) antisense probe for *Grp* (bases 149-707 of *Grp* mRNA, NCBI accession NM_175012.4) and *Tac1*. Briefly, on-slide frozen cervical and thoracic DRG sections at 20 µm thickness were incubated with Proteinase K (50 µg/mL) buffer for 10 min, incubated in prehybridization solution for 3 h at 65°C and then incubated with *Grp or Tac1* probe (~2 µg/mL) in hybridization solution overnight at 65°C. After SSC stringency washes and RNase A (0.1 µg/mL for 30 min) incubation, sections were incubated in 0.01 M PBS with 20% sheep serum and 0.1% Tween blocking solution for 3 h and then incubated with anti-digoxigenin antibody conjugated to alkaline phosphatase (0.5 µg/mL, Roche) in blocking solution overnight at 4°C. After washing in PBS with 0.1% Tween, sections were incubated in NBT/BCIP substrate solution at room temperature for 2–16 h for colorimetric detection. Reactions were stopped by washing in 0.5% paraformaldehyde in PBS. Bright field images were taken using a Nikon Eclipse Ti-U microscope with a Nikon DS-Fi2 Camera. ISH-positive and negative neurons were quantified by an observer blinded to the group or genotype using ImageJ (version 1.34 e, NIH Image) as previously described.[13]

Western blot

Cervical and thoracic DRGs were dissected on ice and quickly frozen in −80°C. Samples were removed into a microcentrifuge tube containing ice-cold sample buffer (20 mM Tris-HCl [pH 7.4], 1 mM dithiothreitol, 10 mM NaF, 2 mM Na_3VO_4, 1 mM EDTA, 1 mM EGTA, 5 mM microcystin-LR, and 0.5 mM phenylmethylsulfonyl fluoride), and homogenized by sonication. Homogenates were centrifuged at 12,000 × *g* for 30 min at 4°C. The supernatant was used for analysis. Protein concentration was determined using BCA assay (Thermo Scientific). For each sample, 10 µg of total protein were separated on SDS NuPAGE Bis-Tris 4–12% gels (Life Technology) in MES running buffer (Life Technology) and transferred to polyvinylidene fluoride membrane (Life Technology). The blots were blocked in 5% bovine serum albumin in PBS and 0.1% Tween 20 for 1 h at

room temperature and incubated with rabbit anti-GRP (ImmunoStar, 1:5000), or rabbit anti-Actin (Sigma, 1:50,000) for 16 h at 4°C. This was followed by 1 h incubation in donkey horseradish peroxidase-linked secondary antibodies (Santa Cruz, 1:2500). Immunoblots were developed with the enhanced chemiluminescence reagents (Thermo Scientific). Band intensities were measured using Kodak 1D (version 3.6) and Actin served as internal control for normalization.

Reverse transcription polymerase chain reaction

RT-PCR was performed as previously described.[39] Mice were sacrificed. DRG and spinal cord tissues were quickly dissected and rapidly frozen in dry ice. Total RNA was isolated and genomic DNA was removed in accordance with manufacturer's instructions (RNeasy plus mini kit; QIAGEN). Single-stranded cDNA (total of 20 μL per sample) was synthesized from 1 μg RNA by using High Capacity cDNA Reverse Transcription Kit (Life Technologies). Gene expression of *Grp* and *Tac1* was determined by real-time PCR (StepOnePlus; Applied Biosystems). Specific intron-spanning primers were designed with the NCBI Primer-BLAST. The primers used are:

Actb (NM_007393.3): 5'-TGTTACCAACTGGGACG ACA-3';
5'-GGGGTGTTGAAGGTCTCAAA-3'; amplicon size: 166 bp.
Gapdh (NM_008084.2): 5'-CCCAGCAAGGACACTG AGCAA-3';
5'-TTATGGGGGTCTGGGATGGAAA-3'; amplicon size: 93 bp.
Grp (NM_175012.3): 5'-TGGGCTGTGGGACACT TAAT-3'; 5'-GCTTCTAGGAGGTCCAGCAAA-3'; amplicon size: 146 bp.
Tac1 (NM_009311.2): 5'-GTGGCCCTGTTAAAGGCT CT-3'; 5'-TGCCCATTAGTCCAACAAAGGA-3'; amplicon size: 85 bp.

Real-time PCR was carried out with FastStart Universal SYBR Green Master (Roche Applied Science). All samples were assayed in duplicates. PCR (heating at 95°C for 10 s and 60°C for 30 s) were performed. Data were analyzed using Comparative CT Method (StepOne Software v2.2.2.), and the expression of target mRNA was normalized to the expression of *Actb* and *Gapdh*.

RT-PCR with 2% agarose gel electrophoresis was performed using Taq DNA Polymerase (New England Biolabs) with 2 μL cDNA as a template per reaction. Reactions were optimized by running annealing temperature and cycle gradients with no-RT (ΔRT) and no-template (H_2O) samples as negative controls. The following intron-spanning primer pairs and PCR parameters were used:

Actb: 5'-GATGACGATATCGCTGCGCTGGTCG-3'; 5'-GCCTGTGGTACGACCAGAGGCATACA-3'; amplicon size 447 bp. Parameters: 95°C 5 min, [95°C 40 s, 55°C 40 s, 72°C 40 s] for 21 cycles, 72°C 10 min.
Grp: 5'-AGTCGAGAGCTCTGAGGGTT-3'; 5'-CCCT TGTCGTTGTCCCTTCA-3'; amplicon size 491 bp. Parameters: 95°C 5 min, [95°C 40 s, 61.4°C 40 s, 72°C 40 s] for 35 cycles, 72°C 10 min.
Nppb (): 5'-CTTTATCTGTCACCGCTGGG-3'; 5'-AGGAGGTCTTCCTACAACAACTTC-3'; amplicon size 329 bp. Parameters: 95°C 5 min, [95°C 40 s, 55°C 40 s, 72°C 40 s] for 28 cycles, 72°C 10 min.
Tac1: 5'-GAGAGCAAAGAGCGCCCAG-3'; 5'-AAG AGCCTTTAACAGGGC-3'; amplicon size 329 bp. Parameters: 95°C 5 min, [95°C 40 s, 55°C 40 s, 72°C 40 s] for 24 cycles, 72°C 10 min.

RNA-seq library preparation

Three adult male C57BL/6J mice were sacrificed by decapitation. Cervical and thoracic DRGs were dissected out and snap frozen on dry ice. Total RNA was extracted using RNeasy Plus Micro Kit (Qiagen) following manufacturer's instructions. RNA concentration and quality was examined using Agilent Bioanalyzer Chip. RNA integrity numbers were above 8.50. Library preparation was performed with Epicentre Ribozero Gold kit (Clontech) according to manufacturer's protocol. cDNA was then blunt ended, an A base was added to the 3' ends, followed by the ligation of Illumina sequencing adapters to the ends. Ligated fragments were then amplified for 12 cycles using primers incorporating unique index tags. Fragments were sequenced on an Illumina HiSeq-2500 using single reads extending 50 bases. Sequencing depth was 55-60M reads per sample.

RNA-seq data acquisition, quality control, and processing

RNA-seq reads were aligned to the GRCm38.76 assembly from Ensembl with STAR version 2.0.4 b.[42] Gene counts were derived from the number of uniquely aligned unambiguous reads by Subread:featureCount version 1.4.5. Transcript counts were produced by Sailfish version 0.6.3. Sequencing performance was assessed for total number of aligned reads, total number of uniquely aligned reads, genes and transcripts detected, ribosomal fraction known junction saturation and read distribution over known gene models with RSeQC version 2.3. All gene-level and transcript counts were then imported into the R/Bioconductor package EdgeR and TMM normalized to adjust for differences in library size. Genes or

transcripts not expressed in any sample were excluded from further analysis. Performance of the samples was assessed with a spearman correlation matrix and multi-dimensional scaling plots. Generalized linear models with robust dispersion estimates were created to test for gene/transcript level differential expression. The fit of the trended and tagwise dispersion estimates were then plotted to confirm proper fit of the observed mean to variance relationship where the tagwise dispersions are equivalent to the biological coefficients of variation of each gene. Differentially expressed genes and transcripts were then filtered for FDR adjusted p values less than or equal to 0.05.

To enhance the biological interpretation of the large set of transcripts, grouping of genes/transcripts based on functional similarity was achieved using the R/Bioconductor packages GAGE and Pathview. GAGE and Pathview were also used to perform pathway maps on known signaling and metabolism pathways curated by KEGG.

GRP protein sequences

Amino acid sequences were obtained from NCBI nucleotide database. The following Genbank Accession numbers are for each species:

Mouse: NM_175012.4, Rat: NM_133570.5, Chimpanzee: XM_001142106.3, Human: NM_002091.3, Dog: XM_861026.3, Rabbit: XM_008261475.1, Guinea Pig: XM_003474134.3, Sheep: NM_001009321.1, Cow: NM_001101239.1, Horse: XM_001489303.1, Chicken: NM_001277900.1.

Statistics

Values are reported as the mean ± standard error of the mean (SEM). Statistical analyses were performed using Prism 6 (v6.0 e, GraphPad, San Diego, CA). For comparison between two groups, unpaired or paired two-tailed t test was used. Normality and equal variance tests were performed for all statistical analyses. $p < 0.05$ was considered statistically significant.

Results

GRP antibody specifically detects GRP in DRGs and the spinal cord

GRP is initially translated as a 148 amino acid prepropeptide that is further processed into smaller biologically active peptides comprising 27 ($GRP_{1–27}$) or 10 amino acids ($GRP_{18–27}$).[43] Comparison of $GRP_{18–27}$ across species reveals that GRP is highly conserved across many species with no differences in the last seven amino acids (WAVGHLM) (Table 2), suggesting that this region is important for its function.

Table 2. Comparison of amino acid sequences of $GRP_{18–27}$ across species.

Mouse	GSHWAVGHLM-amide
Rat	GSHWAVGHLM-amide
Chimpanzee	GNHWAVGHLM-amide
Human	GNHWAVGHLM-amide
Guinea Pig	GNHWAVGHLM-amide
Cow	GNHWAVGHLM-amide
Sheep	GNHWAVGHLM-amide
Horse	GNHWAVGHLM-amide
Chicken	GSHWAVGHLM-amide

Blue amino acids are conserved across different peptides or across species. Red mino acids indicate differences.

Table 3. Comparison of amino acid sequences of mouse neuropeptides.

$GRP_{18–27}$	GSHWAVGHLM-amide
Bombesin (toad)	pEQRLGNQWAVGHLM-amide
Neuromedin B	GNLWATGHFM-amide
Substance P	RPKPQQFFGLM-amide

Green amino acids are conserved across different peptides. Red amino acids indicate differences.

Comparison of $GRP_{18–27}$ with bombesin (toad), as well as neuromedin B (NMB) and SP, reveals some distinct regions (Table 3). The majority of the GRP antibodies are raised against the seven amino acids WAVGHLM which are identical between GRP and bombesin. A recent study suggested that the GRP antibody is only specific at high dilution (1:4000), and GRP could not be detected in DRGs.[25] To address the discrepancies between this study and the others, we first repeated IHC using the GRP antibody at 1:500 and 1:1000 dilutions. Consistent with our previous studies,[13,29] at both dilutions, GRP was clearly detected in wild type (WT) dorsal horn (Figure 1(a) and (c)) but nearly absent in *Grp* knockout (KO) (Figure 1(b) and(d)). However, at 1:4000, GRP was nearly undetectable in WT dorsal horn compared to lower dilutions (Figure 1(e)), while staining was again absent in *Grp* KO (Figure 1(f)). In DRG tissues, results were similar to dorsal horn. At 1:500 (Figure 1(g) and (h)) and 1:1000 (Figure 1(i) and (j)), GRP^+ DRG cell bodies were clearly visible in WT but absent in *Grp* KO. At 1:4000 (Figure 1(k) and (l)), GRP^+ DRG cell bodies were not detectable in either WT or *Grp* KO. Based on these results, we conclude that the GRP antibody is specific and capable of detecting GRP in DRG and spinal cord tissues. Our results from different antibody dilutions, though, may vary with different production lots. For

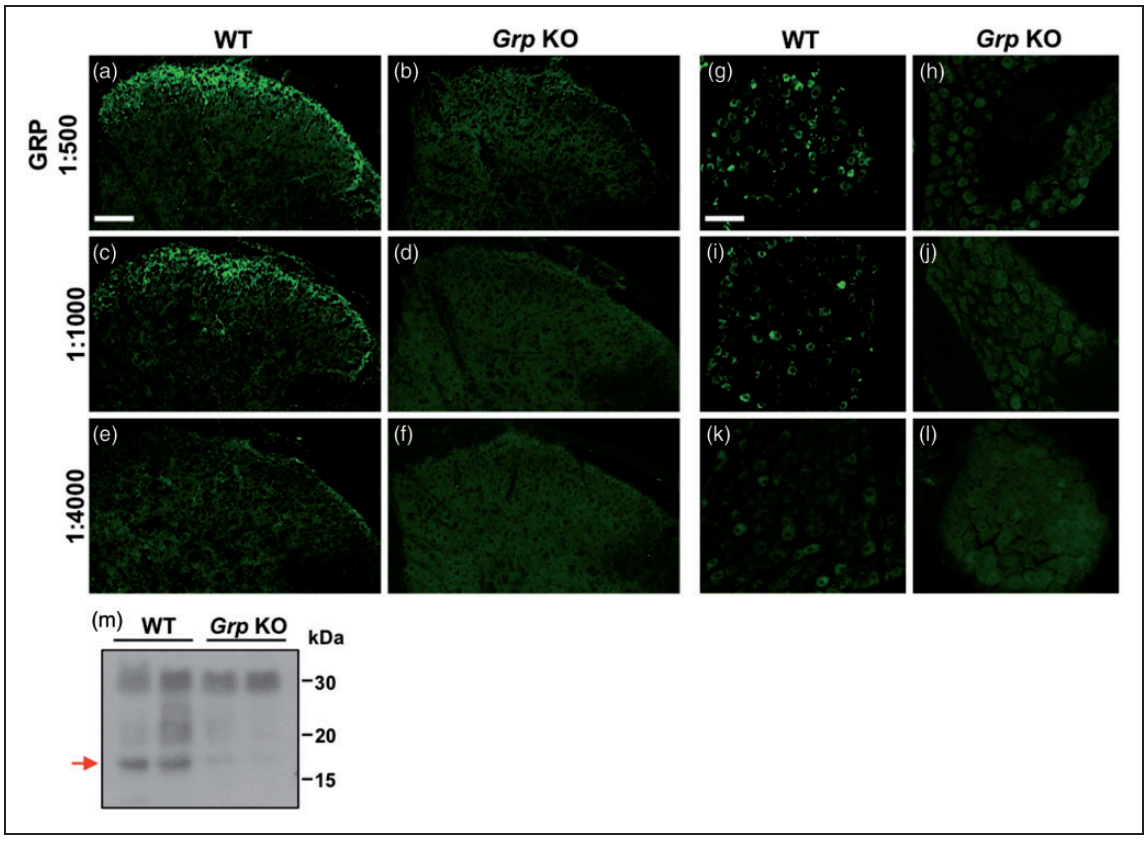

Figure 1. Specific detection of GRP in spinal cord dorsal horn and DRG tissues. (a)–(f) Lumbar dorsal horn IHC images of GRP antibody staining at different dilutions. At 1:500 dilution, GRP is clearly detected in WT (a) but nearly absent in *Grp* KO (b) littermates. At 1:1000 dilution GRP is still detected in WT (c) but absent in *Grp* KO (d). However, at 1:4000 dilution GRP is barely detected in WT (e) and still absent in *Grp* KO (f). (g)–(l), DRG IHC images of GRP antibody at varying dilutions. At 1:500 dilution, GRP^+ DRG neuron cell bodies are clearly detected in WT (g) but almost absent in *Grp* KO (h) littermates. At 1:1000 dilution GRP^+ neurons are still detected in WT (i) but absent in *Grp* KO (j). However, at 1:4000 dilution GRP^+ neurons are barely detected in WT (k) and still absent in *Grp* KO (l). (m) Western blot showed that GRP antibody (1:5000) recognized a band at approximately 16 kDa in WT DRGs, which was not detected in *Grp* KO DRGs. A nonspecific band (~30 kDa) was also shown in all samples. (a)–(l) $n = 3$ mice per genotype and 10 sections per group. (m) $n = 2$ mice per genotype and 20–24 DRGs per animal. Scale bar = 100 μM.

all further staining experiments in this study, we used the 1:1000 dilution.

Many studies have examined GRP expression by IHC, whereas Western blot has not been used. Next, we examined the specificity of the GRP antibody using Western blot analysis of DRG protein homogenates (Figure 1(m)). Although this antibody recognizes several non-specific large sized bands, an approximately 16 kDa band that is equivalent to the size of the full length of GRP prepro-protein was detected in WT but absent in *Grp* KO (Figure 1(m), red arrow). In *Grp* KO tissues, a faint band was visible, but its molecular weight is slightly larger than GRP band in WT and thus considered to be non-specific. These results indicate that the GRP antibody from Immunostar can be used to specifically detect GRP in DRGs by Western blot.

Ablation of primary afferent terminals in the dorsal horn eliminates most of GRP protein

Conflicting results have been reported concerning the expression of GRP protein in DRGs: Fleming et al.[28] showed that the GRP antibody is specific at 1:500 dilution with approximately 2% of DRGs positive for GRP, while Solorzano et al.[25] indicated otherwise. Moreover, an earlier study showed that intrathecal capsaicin injection not only ablated $TRPV1^+$ afferents but also ablated GRP^+ afferents in the dorsal horn,[5] whereas the Solorzano et al.[25] study did not indicate any difference in GRP staining in the dorsal horn following capsaicin injection.

To further investigate the origin of GRP in dorsal horn, mice were intrathecally injected with

resiniferatoxin (RTX), a potent TRPV1 agonist, to ablate TRPV1$^+$ afferents. Previous studies have demonstrated that RTX reliably ablates TRPV1$^+$ afferents, while not affecting TRPV1$^+$ DRG cell bodies.[36] Because approximately 80% of GRP$^+$ DRG neurons express TRPV1,[16] RTX-injection should abolish most of the GRP staining in dorsal horn. Quantitative analysis of TRPV1 staining confirmed almost complete ablation of TRPV1$^+$ afferents in dorsal horn of RTX-injected mice compared to saline-injected control (Figure 2(a)–(c)). Similarly, GRP staining within the same section was nearly abolished in the dorsal horn of RTX-injected mice (Figure 2(d)–(f)). Double IHC images showed an overlap in expression of TRPV1 and GRP in control mice that is eliminated by RTX ablation of TRPV1$^+$ afferents (Figure 2(g) and (h)).

Four independent groups have recently used dorsal rhizotomy of the lumbar spinal cord to evaluate the origin of GRPergic fibers in mice and rats and reported conflicting results.[13,16,18,25,28] Given the inconsistencies and the importance of a complete surgery, it is important to show images of the entire section of the lumbar dorsal horn, both ipsilateral and contralateral sides, a gold standard in the field. It is worth noting that two of these studies that supported the majority of GRP as being derived from the dorsal horn did not show the entire section of the spinal cord, making their results difficult to evaluate and interpret.[25,28] In contrast, we and other researchers showed consistent findings in the spinal cord of mice and rats.[13,18] To further improve the quality of immunostaining for evaluation and to see if our previous finding could be reproduced, one person from our lab performed unilateral rhizotomy, whereas another person carried out double IHC studies on the spinal cord sections. CGRP staining demonstrated almost complete ablation of CGRP$^+$ afferents in the ipsilateral dorsal horn compared to contralateral (Figure 2(i) and (j)), suggesting efficient rhizotomy. Consistent with recent studies in mice and rats,[13,18] GRP staining within the same section was also nearly abolished (Figure 2(k) and (l)). Merged GRP/CGRP image showed significant overlap in expression that is lost in the ipsilateral dorsal horn (Figure 2(m)). Taken together, the RTX-mediated TRPV1 fiber ablation and rhizotomy results support the notion that most of GRP, as well as TRPV1 and CGRP, in the dorsal horn is of primary afferent origin. It cannot be excluded, though, that small amounts of these peptides and channels in the dorsal horn may originate from spinal cord interneurons or from other sources such as descending projections. For example, previous studies suggested that GRP is expressed in neurons of the lateral parabrachial nucleus,[44] a region which has been shown to project directly to the spinal cord dorsal horn.[45]

GRP is detectable in DRG, but not dorsal horn, primary cultures

To examine if there are GRP$^+$ neurons in the dorsal horn, we dissected out DRGs and dorsal horn of the spinal cord, acutely dissociated DRG and dorsal horn neurons and cultured the neurons for GRP and NeuN double IHC (Figure 3(a)). We found that about 3.8% (6/157) of NeuN$^+$ DRG neurons were GRP$^+$ (Figure 3(b)). However, we were unable to find any GRP$^+$ dorsal horn neurons (Figure 3(b)). These results suggest that GRP protein is not expressed in dorsal horn neurons or the expression level falls below the detectable limit.

GRP expression partially, but not completely, overlaps with substance P in DRG neurons

Although GRP and NMB share five of the seven amino acids in their C-terminal regions (Table 3), several pieces of evidence indicate that the GRP antibody does not recognize NMB: despite overlapping expression, NMB is also detected in non-peptidergic neurons.[40] In contrast, SP only has homology with GRP in the last two amino acids (Table 3), with the last one, methionine (M) shared by many neuropeptides. Thus, it is unlikely that one amino acid would make the GRP antibody recognize only SP even though there is cross-reactivity. Indeed, it has been demonstrated that GRP and SP antibodies also recognized neurons singularly expressing either SP or GRP.[3,18]

We revisited this issue by performing double IHC on DRG neurons from WT and Grp KO mice (Figure 4). Both GRP (Figure 4(a)) and SP (Figure 4(c)) were detected in the subset of WT DRG neurons. In contrast, while GRP was absent in *Grp* KO mice (Figure 4(b)), SP expression was not affected in *Grp* KO mice (Figure 4(d)). Merged images (Figure 4(e) and (f)) show that about approximately 50% of GRP$^+$ neurons are SP$^+$ in WT DRG. A Venn diagram further illustrates the GRP and SP neuron overlap and percentages in WT DRGs (Figure 4(g)). Consistent with previous studies,[13,16] the percentage of GRP$^+$ neurons was approximately 8%, whereas the percentage of SP$^+$ neurons was approximately 12.5% of the total.

GRP$^+$ and SP$^+$ terminals make contacts with GRPR$^+$ neurons in dorsal horn

To examine whether SP$^+$ or GRP$^+$ terminals make connections with GRPR$^+$ neurons in the spinal dorsal cord, triple IHC was performed for SP, eGFP, and GRP in GRPR-eGFP mice. Some GRPR$^+$ neurons and densely SP$^+$ and GRP$^+$ terminals were found in the superficial part (laminae I and IIo) of the spinal dorsal horn (Figure 5(a)–(c)). Many SP$^+$ or GRP$^+$ fibers could be observed making contacts with GRPR$^+$ neurons

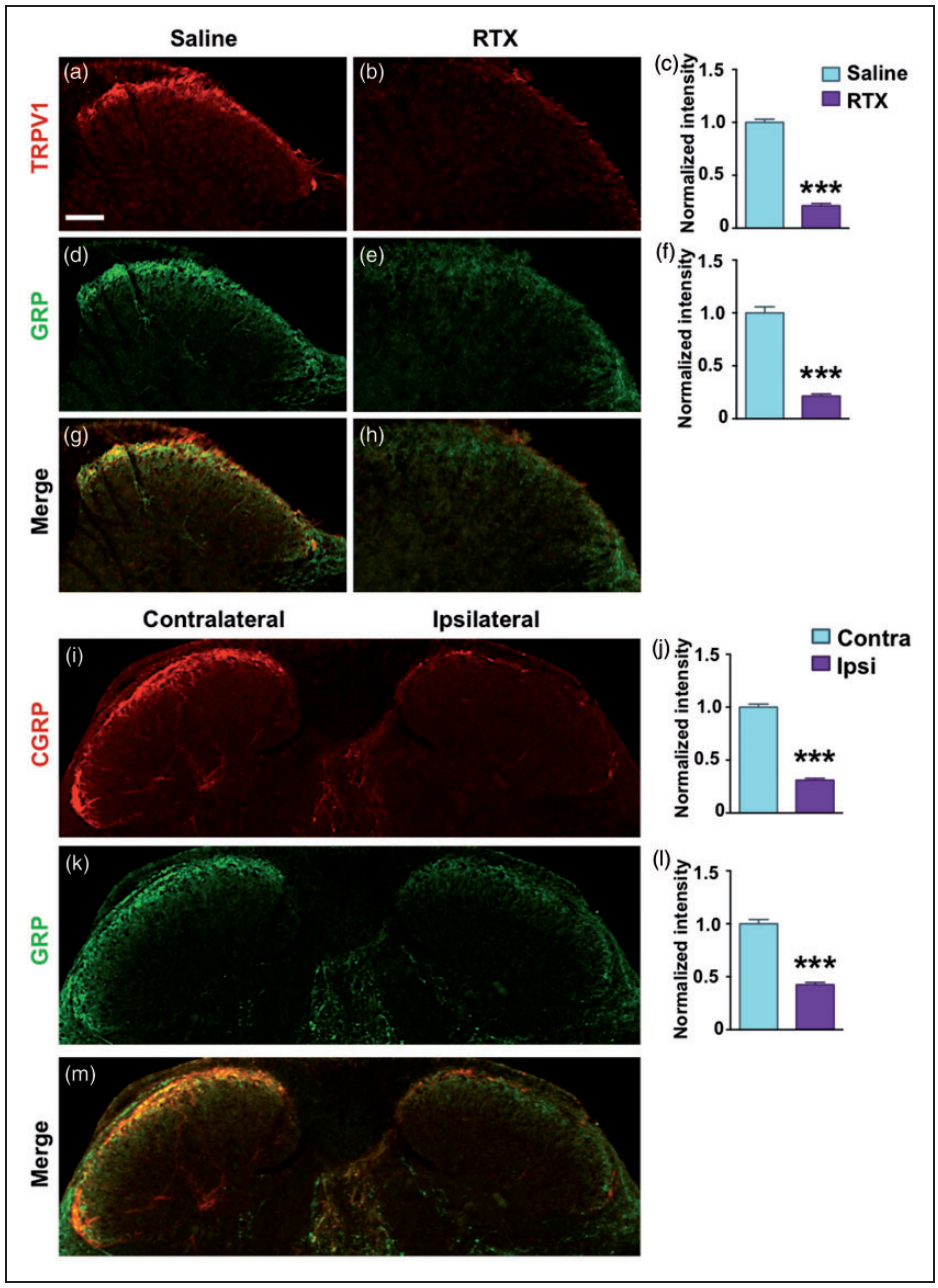

Figure 2. Chemical or surgical ablation of primary afferent terminals eliminates most of GRP protein in the dorsal horn. (a)–(c) Lumbar dorsal horn IHC images of TRPV1 staining from mice injected intrathecally with saline (a) or RTX (25 ng) (b) and normalized intensities (c) indicate near complete ablation of TRPV1 signal in RTX-treated mice. (d)–(f) Comparison of GRP staining images from saline (d) and RTX (e) groups and intensities (f) also show almost total ablation of GRP signal in RTX-treated mice. (g, h) Merged images indicate most GRP staining overlaps with TRPV1 in saline control (g) which is mostly absent in RTX-treated mice (h). (i, j) A single lumbar dorsal horn image of CGRP staining from dorsal rhizotomy mice of both contralateral and ipsilateral sides of the surgery (i) and normalized intensities of each side (j) shows that rhizotomy eliminated nearly all CGRP signal in the ipsilateral side. (k, l) GRP staining image of rhizotomy contra- and ipsilateral dorsal horn (k) and intensities (l) indicates an almost complete ablation of GRP signal in ipsilateral side compared with contralateral. (m) Merged image shows significant overlap in GRP and CGRP staining in contralateral side that is eliminated in ipsilateral side following rhizotomy. Scale bar = 100 μM. Data are presented as mean ± SEM. $n = 3$ mice per group and 10 sections per group. Unpaired *t* test in (c) and (f). Paired *t* test in (j), and (l), ***$p < 0.001$.

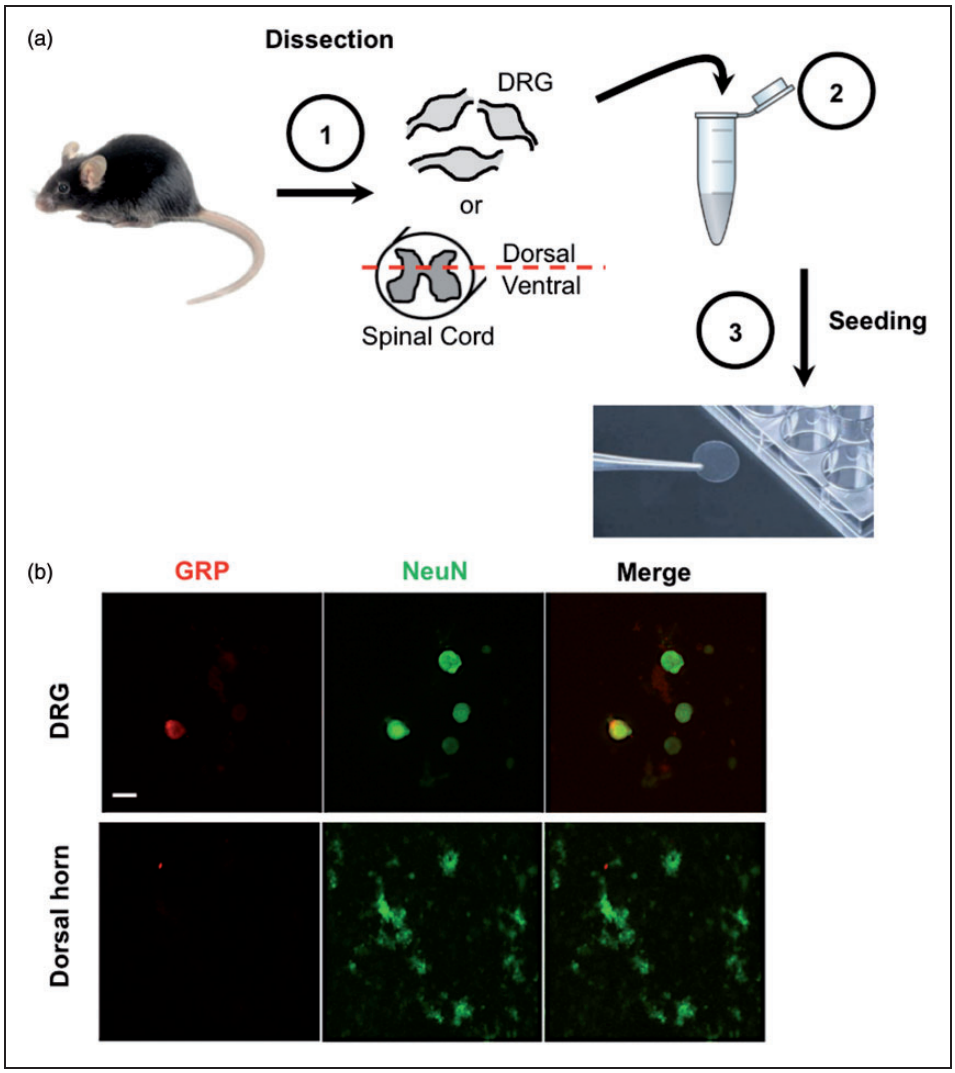

Figure 3. Detection of GRP in acutely dissociated DRG neurons, but not dorsal horn neurons. (a) Illustration of DRG and dorsal horn dissection and culture process. (b) IHC of acutely dissociated DRG neurons (upper row) and spinal dorsal horn neurons (lower row) using rabbit anti-GRP (1:1000). Scale bar, 20 μm.

(Figure 5(d)–(f)), and a few SP and GRP double-labeled terminals could be found making contacts with $GRPR^+$ neurons (Figure 5(f)).

To examine the colocalization of SP and GRP in the spinal dorsal horn, double immuno-electron microscopic (Immuno-EM) for SP and GRP were performed in the lumbar cord. Some SP^+ terminals identified by the silver-enhanced nanogold particles enhancement are colocalized with GRP^+ terminals revealed by the immunoperoxidase reaction products (Figure 5(g)), and some axon terminals only express GRP (Figure 5(h)) or SP (not shown). SP^+ or GRP^+ terminals formed asymmetric synapses with $GRPR^+$ dendritic profiles (Figure 5(i)–(k)), and more GRP^+ fibers formed synaptic connections with $GRPR^+$ neurons than SP^+ fibers (~2:1 GRP:SP contacts with GRPR neurons). Although a majority of GRP^+ fibers in the dorsal horn are of primary afferent origin, it cannot be excluded that some of the GRP-GRPR and SP-GRPR contacts in the dorsal horn may be due to GRP^+ or SP^+ descending projections from the brain as mentioned earlier.

Genetic deletion of Tac1 results in reduced peptidergic expression in spinal cord dorsal horn

The *Tac1* gene encodes the propeptide that is cleaved to generate SP and three other neuropeptides of the tachykinin family.[46] Solorzano et al.[25] showed that GRP expression is reduced in the spinal cord of *Tac1* KO mice, which was interpreted as evidence for a presumed lack of specificity of the GRP antibody. Because *Tac1* KO mice also exhibited deficits in expression of other antibody immunostaining,[47,48] we speculated that an attenuated GRP expression may reflect broader abnormalities of gene expression in the primary afferents of *Tac1* KO mice.

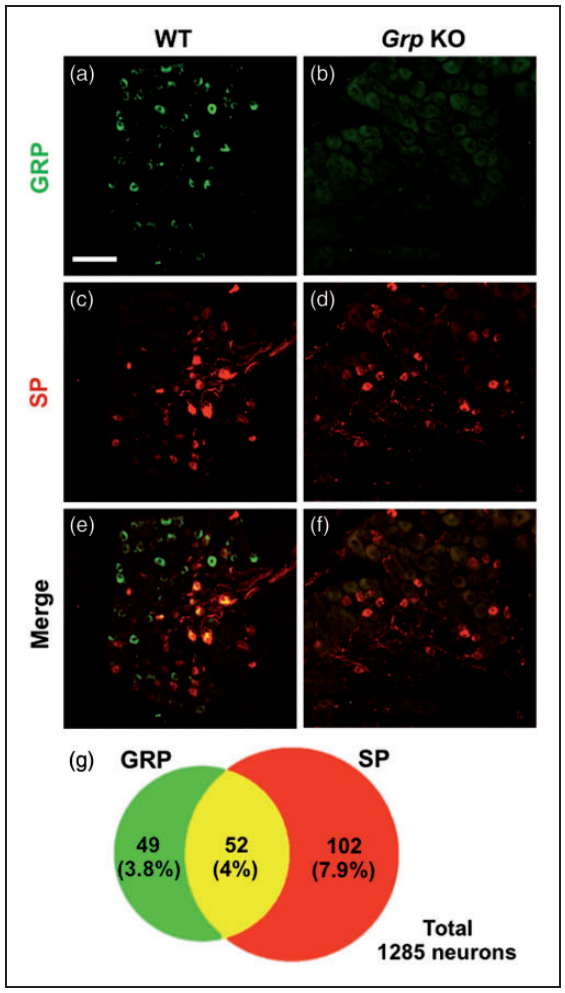

Figure 4. GRP expression partially, but not completely, overlaps with Substance P in DRG neurons. (a)–(f) Double IHC of DRG sections was performed in *Grp* WT and KO mice. Images of sections stained with GRP in *Grp* WT (a) and *Grp* KO (b). Images of sections stained with SP in *Grp* WT (c), and *Grp* KO (d). Merged images of GRP-SP staining in *Grp* WT (e) and *Grp* KO (f). (g) Venn diagram of GRP-SP expression overlap in DRG. Green is GRP^+-only neurons, red is SP^+-only neurons, and yellow is GRP^+-SP^+ neurons. Scale bar = 100 μm. $n = 3$ mice and 10 sections per genotype.

To examine whether lack of SP may influence expression of other molecular markers, we performed IHC staining in spinal dorsal horn sections from WT and *Tac1* KO littermates. As expected, SP staining was absent in *Tac1* KO dorsal horn (Figure 6(a)–(c)). Consistent with previous results,[25] GRP staining was significantly reduced in *Tac1* KO compared to WT (Figure 6(d)–(f)). Remarkably, a small reduction, yet significant, was observed for CGRP staining (Figure 6(g)–(i)), and NPY staining was dramatically reduced (Figure 6(j)–(l)) in *Tac1* KO relative to the control. However, the non-peptidergic IB4-binding pattern and intensity was similar in WT and *Tac1* KO dorsal horn (Figure 6(m)–(o)). Taken together, these results suggest that *Tac1* is important for either expression and/or trafficking of neuropeptides in peptidergic primary afferents.

Optimized methods for detection of GRP in DRG

Considerable variations of GRP immunostaining have been observed in DRG neurons, ranging from somewhat widespread GRP staining[25–27,29] to more distinct or restricted staining.[3,13,16,18,28] One study even described two types of GRP neurons comprising low and high level of expression.[19] We compared two different staining methods: either mounted on slides prior to antibody incubation,[25] or sections stained floating freely in PBS, and mounted after staining. Using the same antibody, on-slide staining resulted in a widespread staining pattern for GRP (Figure 7(a)), whereas free-floating staining of DRG sections revealed a more distinct and specific pattern (Figure 7(b)). These results suggest that the discrepancies can be attributed to differences in IHC protocols rather than insufficient antibody specificity.

Concerning *Grp* mRNA expression in DRG, a few studies reported negative ISH results,[25,28,30] while our recent study showed detectable ISH signal for *Grp* in WT DRG neurons,[12] which is comparable to GRP IHC staining pattern. To optimize the methods for reliable *Grp* mRNA detection, we tested different incubation times for color development of *Grp* ISH signals on WT DRG sections. Grp^+ signals were barely detectable after 4 h of incubation in NBT/BCIP colorimetric substrate (Figure 7(c), arrows), but continuing incubation to 16 h produced specific Grp^+ signals (Figure 7(d), arrowheads). The fact that detection of *Grp* signals by ISH requires a longer incubation time for color development than most other probes suggests that *Grp* transcripts are likely present in low copy number, rendering them difficult to detect by conventional protocols.

We next performed molecular expression analyses by RNA-seq in DRGs from adult mice. Read length was set at 50 bases with a sequencing depth in a range of 55–60 million single end reads to allow detection of low-abundance transcripts such as *Grp*, according to the ENCODE Consortium's "Standards, Guidelines and Best Practices for RNA-seq" (https://genome.ucsc.edu/ENCODE/protocols/dataStandards/ENCODE_RNAseq_Standards_V1.0.pdf). Transcript abundance is expressed as FPKM (Fragments Per Kilobase of transcript per Million fragments mapped), which provides a length and depth normalization to permit comparisons both within and between samples.[49] In this condition, we detected the level of *Grp* transcripts in WT DRGs as 0.27 ± 0.0033 FPKM, which is lower than the level of *Npy* (1.91 ± 0.47 FPKM), *Mrgpra3* (3.87 ± 0.85 FPKM), *Tac1* (18.45 ± 2.42 FPKM), and *Nmb* (48.81 ± 9.33 FPKM) but very close to the level of *Pdyn*

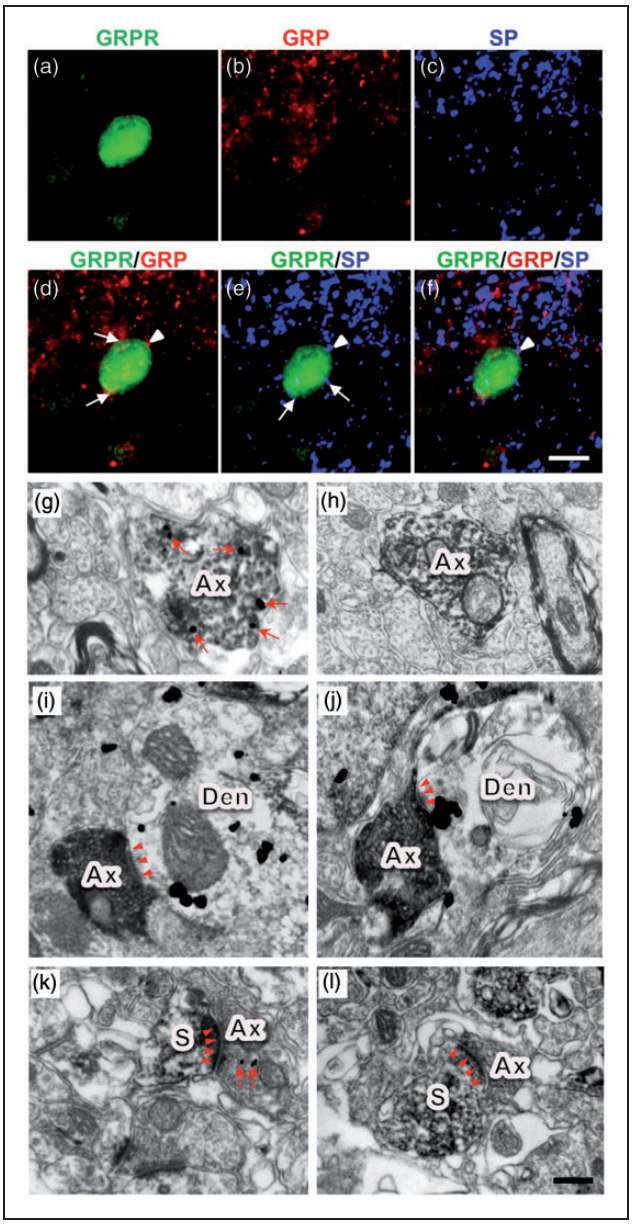

Figure 5. GRP^+ and SP^+ fibers contacts on $GRPR^+$ neurons in the superficial spinal dorsal horn. (a)–(c) Triple immunostaining of an $eGFP^+$ neuron (a), GRP^+ (b), and SP^+ (c) fibers in the superficial spinal dorsal horn. (d) Merged image of (a) and (b) showing GRP^+ fibers (arrows and arrowhead) contact with the GFP^+ GRPR neuron. (e) Merged image of (a) and (c) showing SP^+ fibers (arrows and arrowhead) contact with the GFP^+ GRPR neuron. (f) Merged image of (a), (b) and (c) showing close contacts between SP^+/GRP^+ colocalized fibers (arrowhead) and the GFP^+ GRPR neuronal cell body. Scale bar = 10 μm for (a)–(f). (g)–(l), EM images of SP^+, GRP^+, and $GRPR^+$ ultrastructures. (g), SP^+ (arrows, silver grains) and GRP^+ (DAB reaction products) labels are colocalized in the same axon terminal (Ax). (h), A GRP^+ (DAB reaction products) single labeled axon terminal (Ax). SP^+ axon terminal (Ax; DAB reaction products) makes asymmetric synaptic contacts with $GRPR^+$ dendritic profiles (Den; silver grains) (i, j). GRP^+ (k; silver grains) and GRP^- (l; no positive production) axon terminals (Ax) make asymmetric synaptic contacts with $GRPR^+$ dendritic profiles (Den; DAB reaction products). Arrowheads indicate postsynaptic membranes. Scale bar = 0.2 μm for (g)–(l).

(0.13 ± 0.059 FPKM), *Hrh1* (0.20 ± 0.023 FPKM), and *Mrgprx1* (0.57 ± 0.13 FPKM) (Table 4). Thus, *Grp* transcripts in mouse DRGs can be detected by RNA-seq. Moreover, its expression is even lower than *Npy*, a gene whose mRNA expression often falls below the threshold of detection by conventional ISH technique.

Finally, we performed RT-PCR followed by gel electrophoresis to further analyze the abundance of *Grp* transcripts in intact DRGs, as *Grp* became detectable only at ⩾32 cycles (Figure 7(e)), whereas *Nppb*, which encodes B-type neuropeptide and *Actb* were observed after 26 and 18 cycles, respectively (Figure 7(e)). This

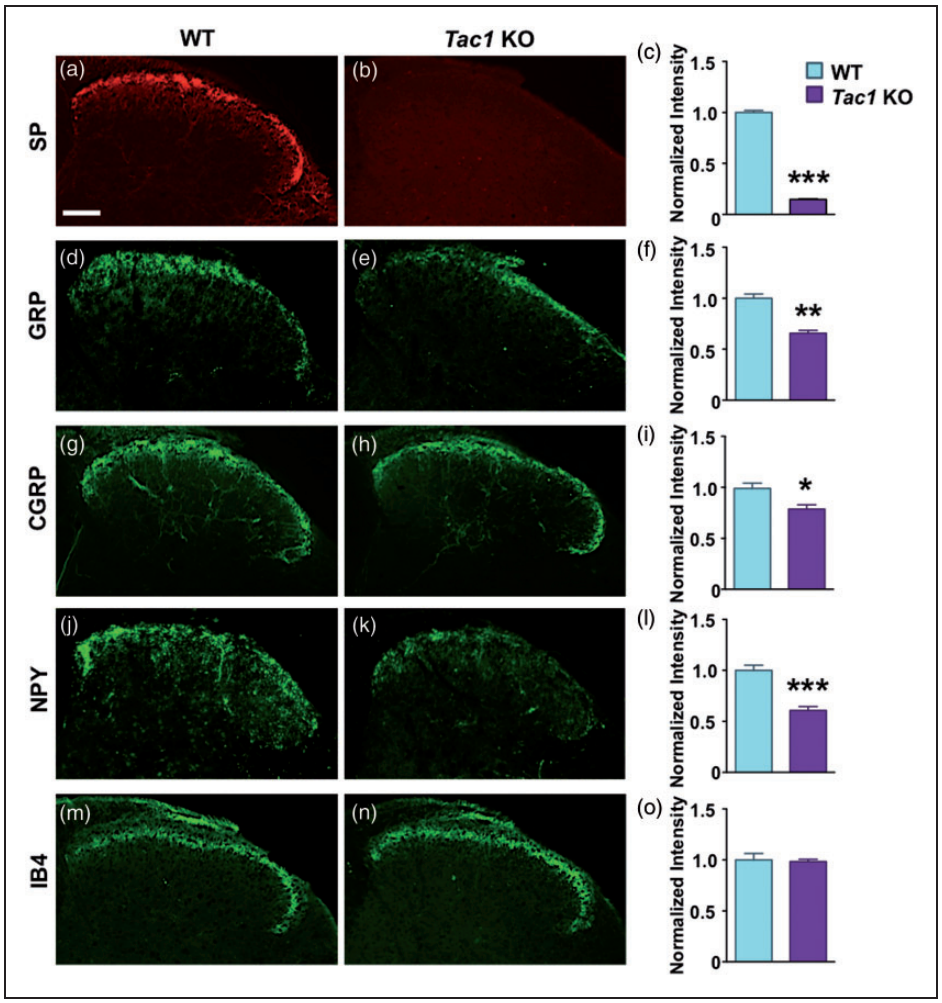

Figure 6. Apparent reduction of peptidergic markers in dorsal horn of *Tac1* gene-deleted mice. (a)–(c) Lumbar dorsal horn IHC images of SP staining in WT (a) and *Tac1* KO (b) and normalized intensities (c) show loss of SP expression. (d)–(f) IHC images of GRP staining in WT (d) and *Tac1* KO (e) with normalized intensities (f) indicate a significant reduction in GRP signal in *Tac1* KO. (g)–(i) CGRP staining images in WT (g) and *Tac1* KO (h) with intensities (i) also show a small, but significant, reduction in CGRP in *Tac1* KO. (j)–(l), NPY staining images in WT (g) and *Tac1* KO (h) with intensities (i) indicates a large reduction in NPY signal in *Tac1* KO. (m)–(o) IB4-binding images in WT (m) and *Tac1* KO (n) with intensities (o) show no apparent differences. Scale bar = 100 μM. Data are presented as mean ± SEM. n = 3 mice per genotype and 10 sections per group. Unpaired *t*-test in (c), (f), (i), and (l), $*p < 0.05$, $**p < 0.01$, $***p < 0.001$.

finding is consistent with previous studies[28,30] and confirmed the presence of *Grp* mRNA in uncultured DRGs. It also underscores the fact that sufficient PCR cycles are required for *Grp* detection.

Increased numbers of Grp$^+$, but not Tac1$^+$, neurons and upregulation of Grp mRNA levels in dry skin-induced chronic itch DRGs

SP-NK1R signaling has been implicated in itch transmission and development of chronic itch.[23,50,51] However, it remains unclear whether *Tac1*/SP expression in DRG increases in chronic itch conditions. Therefore, we used the AEW dry skin mouse model of chronic itch model to assess the effects of chronic itch on *Tac1* mRNA expression in DRG. *Grp* expression was absent in *Grp* KO neurons (Figure 8(a)) demonstrating that the probe is specific for *Grp*. Consistent with our previous studies,[12] the percentage of *Grp*$^+$ neurons was almost doubled in DRG from dry skin mice compared to water-treated control (Figure 8(b)–(d)). In contrast, the percentage of *Tac1*$^+$ neurons, which was unaffected in *Grp* KO (Figure 8(e)), was comparable in DRG between dry skin and the control mice (Figure 8(f)–(h)). Lastly, we performed RT-PCR with gel electrophoresis to visualize *Grp* and *Tac1* mRNA expression with *Actb* as control, which clearly showed increased band intensities for *Grp* in dry skin mice, whereas *Tac1* in dry skin appeared similar to control (Figure 8(i)). qRT-PCR was also performed that showed Grp

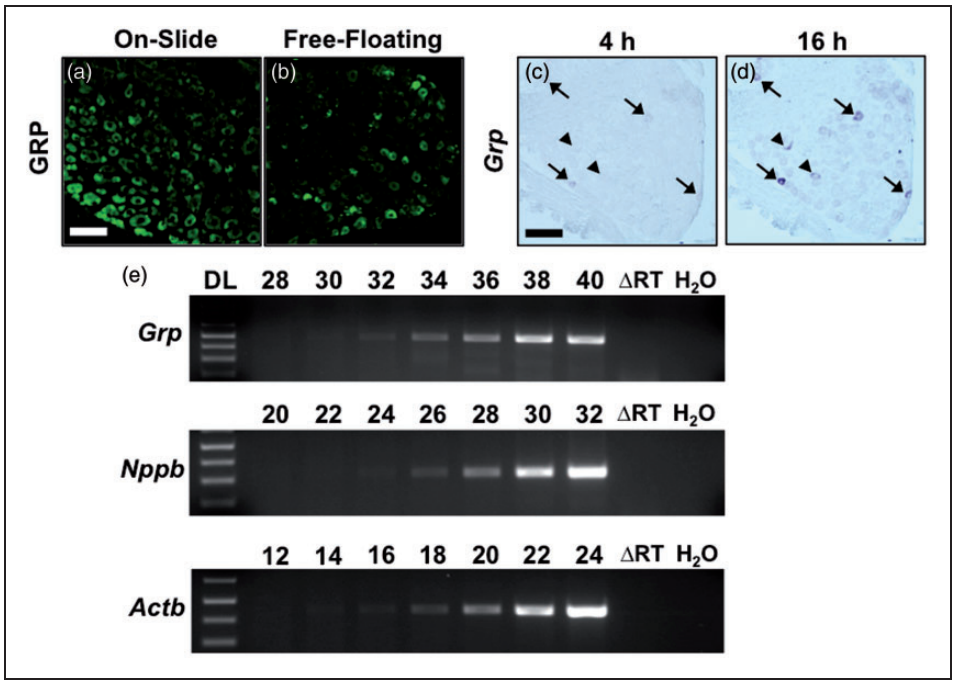

Figure 7. Optimized methods for GRP detection in DRG. (a, b) IHC images of GRP antibody (1:1000) from DRG on-slide section (a) and free-floating section (b). (c, d) ISH images of DRG section incubated in NBT/BCIP substrate for 4 h (**c**) and 16 h (d). Arrows indicate Grp^+ neurons that were barely detected at 4 h. Arrowheads indicated Grp^+ neurons that were detected after incubation of 16 h but not 4 h. (e) Gel electrophoresis of *Grp* (upper image), *Nppb* (middle image) and *Actb* (lower image) RT-PCR products from DRGs using cycle gradient. For no RT sample (ΔRT), reverse transcriptase was not added to RNA to amplify cDNA. For water sample, no cDNA was added to reaction. DL, DNA ladder. Scale bar = 100 μM.

Table 4. Gene expression level in DRGs as detected by RNA-Seq.

Table 4. Gene expression level in DRGs as detected by RNA-Seq

	Mouse 01	Mouse 02	Mouse 03	Mean ± SEM
Pdyn	0.10	0.042	0.24	**0.13 ± 0.059**
Hrh1	0.19	0.16	0.24	**0.20 ± 0.023**
Grp	0.27	0.28	0.27	**0.27 ± 0.0033**
Mrgprx1	0.77	0.61	0.34	**0.57 ± 0.13**
Npy	1.95	1.07	2.71	**1.91 ± 0.47**
Mrgpra3	3.92	5.31	2.37	**3.87 ± 0.85**
Tac1	20.30	21.40	13.65	**18.45 ± 2.42**
Nmb	45.10	67.08	34.26	**48.81 ± 9.66**
Actb	347.31	410.05	421.66	**393.00 ± 23.09**

FPKM 0 5 50

expression was increased approximately seven fold in DRG from dry skin mice compared to control (Figure 8(j)). A smaller, albeit statistically significant, approximately 1.2 fold increase was detected for *Tac1* expression in dry skin DRG by qRT-PCR (Figure 8(k)).

Dry skin-induced chronic itch in mice increases the numbers of GRP, but not SP, positive neurons in the DRG

Next, double IHC was performed to examine SP and GRP expression in DRG sections of mice with dry skin

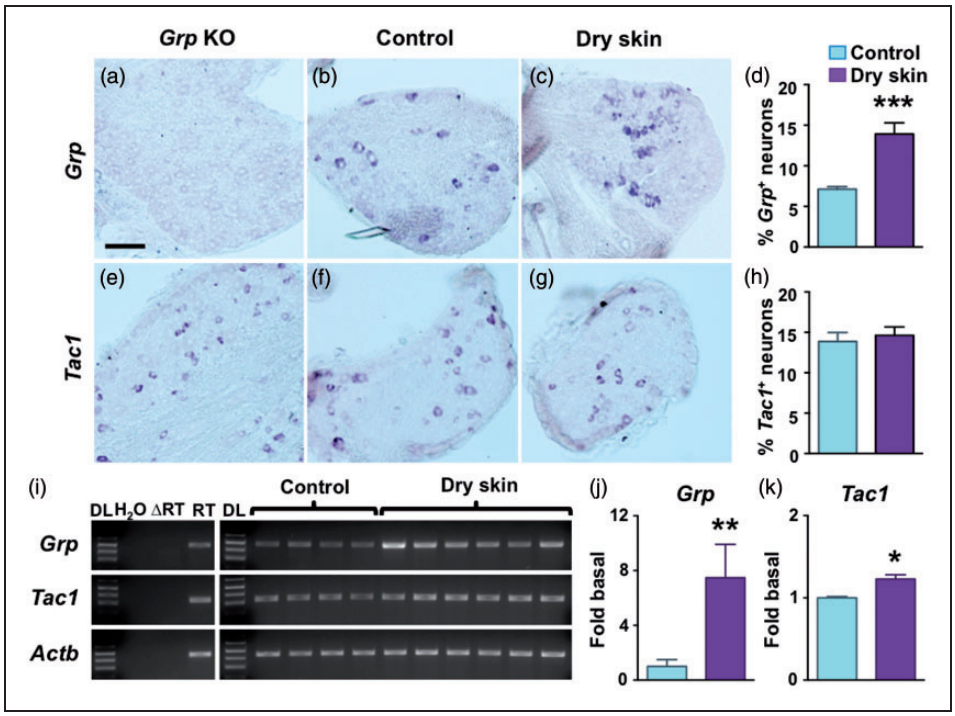

Figure 8. Increased *Grp*$^+$, but not *Tac1*$^+$, neurons and upregulation of *Grp* mRNA levels in Dry skin-induced chronic itch DRGs. (a)–(d) Cervical DRG images of *Grp* ISH. *Grp* ISH is absent in *Grp* KO (a). Comparison of control (b) and dry skin (c) DRG indicates the percentage of *Grp*$^+$ neurons is nearly doubled in dry skin mice (d). (e)–(h) Cervical DRG images of *Tac1* ISH. *Tac1* ISH is unaffected in *Grp* KO (e). Comparison of *Tac1* ISH from control (f) and dry skin (g) shows no significant difference in percentage of *Tac1*$^+$ neurons in DRG (h). (i) Gel electrophoresis images of RT-PCR products also shows an increase of *Grp* mRNA in dry skin DRG samples compared to control and, whereas *Tac1* mRNA increase in dry skin DRG is less apparent and *Actb* levels appear similar between the two groups. No products were detected in H_2O and no-RT (ΔRT) samples, whereas RT samples had a single band detected for each mRNA. DL, DNA ladder. (j, k) Quantitative RT-PCR results from control and dry skin DRG show a approximately 7 fold increase in *Grp* mRNA levels (**j**) and a approximately 1.2 fold increase in *Tac1* mRNA levels (**k**) in dry skin. Scale bar = 100 μM. Data are presented as mean ± SEM. $n = 3$ mice per group and 10–12 DRG sections per group in. $n = 4$–6 mice per group and 20–24 DRGs per animal in **i-k**. Unpaired *t*-test in **d**, **h**, **j**, and **k**. * $p < 0.05$, ** $p < 0.01$, *** $p < 0.001$.

itch. Compared to water-treated control (Figure 9(a)), the percentage of GRP$^+$ neurons in DRG was nearly doubled in dry skin-induced chronic itch (Figure 9(b) and (c)), consistent with the results from *Grp* ISH. Also consistent with *Tac1* ISH, the percentage of SP$^+$ neurons was similar in dry skin-induced chronic itch DRG compared to control (Figure 9(d)–(f)). Merged images (Figure 9(g) and (h)) indicate no significant difference in the percentage of double-positive neurons in dry skin mice compared to control (Figure 9(i)) suggesting ectopic expression of GRP in non-SP DRG neurons in chronic itch. To further confirm the immunostaining results, Western blot of DRG protein extracts was performed using the GRP antibody (Figure 9(j) and (k)). Western blot of dry skin DRG protein samples indicated an apparent upregulation of GRP levels compared to control (Figure 9(j)), and quantitative analysis showed significant increase of GRP in dry skin DRGs (Figure 9(k)). Taken together, these data confirm previous results that GRP protein is upregulated in chronic itch,[12,13] whereas SP is not increased in chronic itch. There are conflicting reports of SP expression related to chronic itch. Some studies reported increases in SP skin fibers and mast cells in human atopic dermatitis (AD) skin and mouse AD models,[51–53] whereas other studies found reduced SP in AD skin.[54,55] However, to our knowledge, no other studies have investigated SP expression in DRG in dry skin-induced chronic itch conditions. Our findings suggest that in dry skin-induced chronic itch, SP expression in DRG is largely unaffected.

Neither Grp nor Tac1 expression are increased in dorsal horn of mice with dry skin-induced chronic itch

While it is clear that *Grp* expression in DRG is upregulated during chronic itch, the effect of chronic itch on *Grp* expression in the dorsal horn has not be investigated. This issue is important because, assuming *Grp*$^+$ dorsal horn neurons are important for chronic itch, one would anticipate an upregulation of *Grp* mRNA in the spinal cord of mice with dry skin itch. To examine this, we performed *Grp* and *Tac1* ISH and found that the

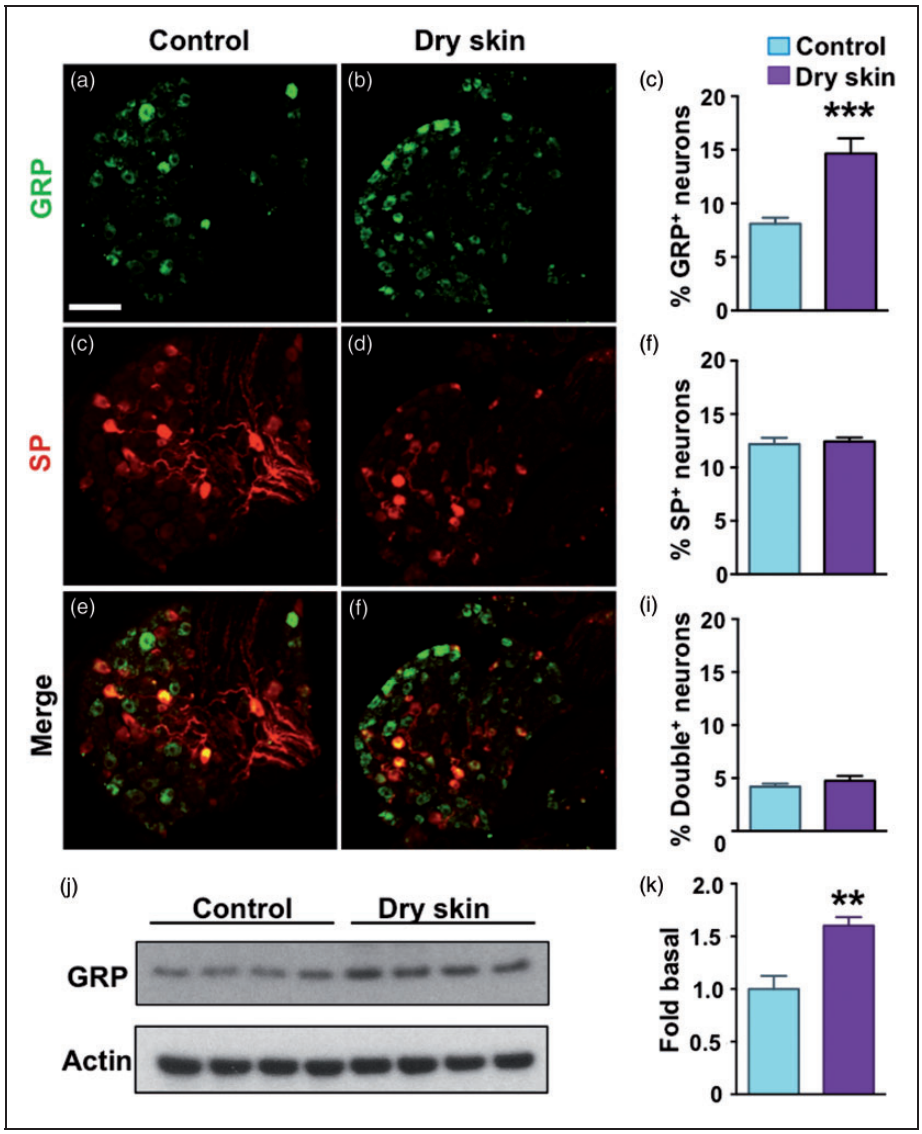

Figure 9. Dry skin-induced chronic itch increases GRP^+, but not SP^+, neurons in DRG. (a)–(c) Cervical DRG images of GRP staining. Comparison of GRP staining from water-treated control (a) and AEW-treated dry skin mice (b) shows the percentage of GRP^+ neurons in DRG is nearly doubled in dry skin mice (c). (d)–(f) DRG images of SP staining. Comparison of SP staining from water-treated control (d) and AEW-treated mice (e) shows no significant difference in percentage of SP^+ neurons in DRG (f). (g)–(i) Merged images of GRP and SP staining. Image from control (g) and dry skin (h) indicates some overlap in GRP and SP expression in DRG, yet the percentage of $Double^+$ neurons is not increased in DRG from dry skin mice (i). (j) (k) Western blot (j) and quantified data (k) showed that GRP protein level was significantly upregulated ($p = 0.0066$) in DRGs of dry skin mice comparing to that of control mice. Scale bar = 100 μM. $n = 3$ mice per group and 10–12 DRG sections per mouse in (a)–(i). $n = 4$ mice per group and 20–24 DRGs per animal in (j) (k). $^{**}p < 0.01$, $^{***}p < 0.001$, unpaired *t* test in (c), (f), (i), and (k).

number of Grp^+ neurons in both cervical and thoracic dorsal horn was similar in dry skin mice and controls (Figure 10(a)–(f)). $Tac1^+$ neuron numbers also appeared unchanged in both cervical and thoracic dorsal horn from dry skin mice compared to controls (Figure 10(g)–(l)). qRT-PCR of cervico-thoracic spinal cord cDNA also revealed no significant differences in *Grp* (Figure 10(m)) or *Tac1* (Figure 10(n)) expression in dry skin mice compared to control.

Discussion

The specificity of the GRP antibody and cross-reactivity with SP

In this study, we show that different IHC protocols could have major effects on the staining outcome even though the same GRP antibody was used. Regardless of the method used, optimization of the procedure is a pre-requisite for performing specific GRP immunostaining,

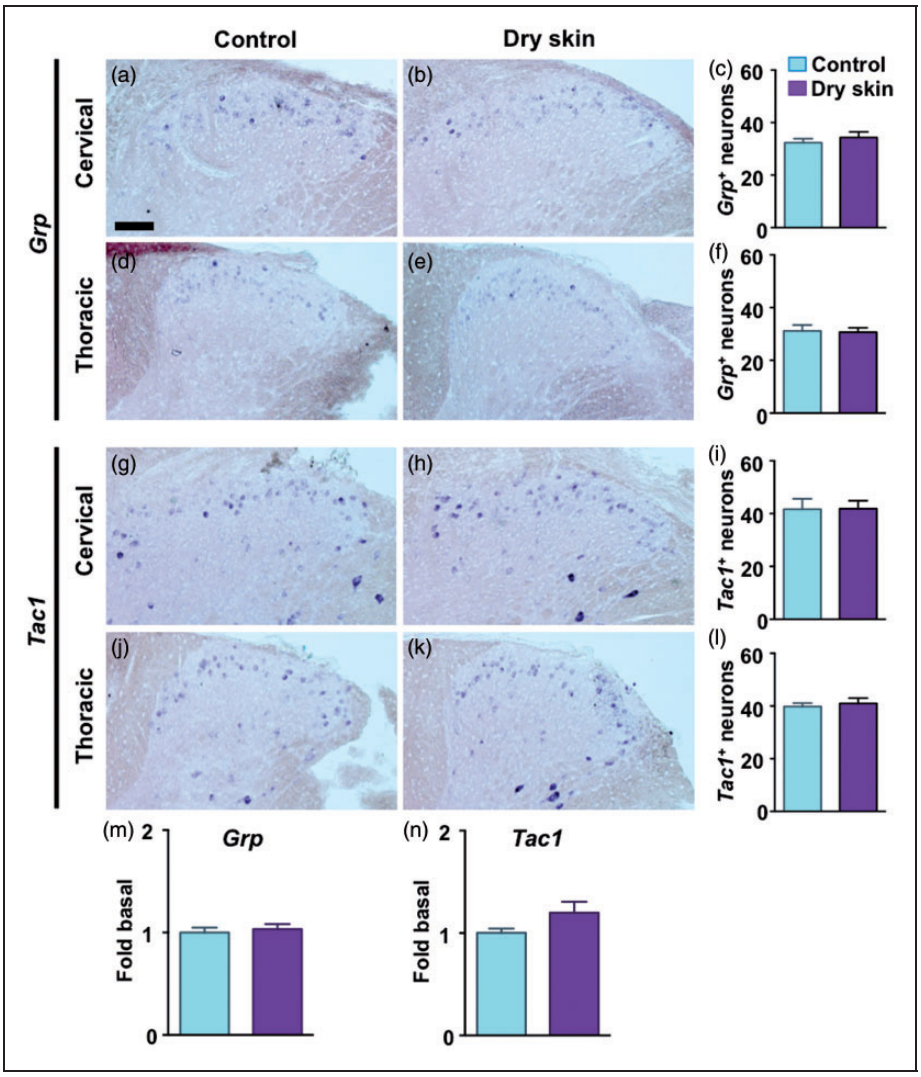

Figure 10. *Grp*$^{+}$ and *Tac1*$^{+}$ neurons, as well as mRNA levels, in the spinal cord are not increased in dry skin-induced chronic itch mice. (a)–(c) Cervical dorsal horn images of *Grp* ISH. Comparison of *Grp* ISH from water-treated control (a) and AEW-treated dry skin (b) shows no significant difference in the number of *Grp*$^{+}$ neurons in cervical region (c). (d)–(f) Thoracic dorsal horn images of *Grp* ISH. Comparison of *Grp* ISH from control (d) and dry skin (e) also shows no significant difference in the number of *Grp*$^{+}$ neurons in thoracic region (f). (g)–(i) Cervical dorsal horn images of *Tac1* ISH. Comparison of *Tac1* ISH from control (g) and dry skin (h) shows no significant difference in the number of *Tac1*$^{+}$ neurons in cervical region (i). (j)–(l) Thoracic dorsal horn images of *Tac1* ISH. Comparison of *Tac1* ISH from control (j) and dry skin (k) also shows no significant difference in the number of *Tac1*$^{+}$ neurons in thoracic region (l). (m) and (n) Quantitative RT-PCR results from control and dry skin cervico-thoracic spinal cord show no significant differences in *Grp* mRNA levels (m) or *Tac1* mRNA levels (n). Scale bar = 100 μM. $n = 3$ mice per group and 10–12 sections per mouse in (a)–(l). $n = 5$ mice per group in (m) and (n). Unpaired *t* test in (c), (f), (i), (l), (m), and (n).

as many pitfalls such as perfusion and the quality of tissues may influence the outcome of IHC.[56] Although the GRP antibody is specific, it remains one of the most difficult antibodies to work with in our experience. This is also true for *Grpr* ISH, as many investigators are unable to detect *Grpr* in the spinal cord. Thus, if distinct GRP immunostaining cannot be achieved in DRG, it would be difficult to interpret the results obtained from spinal cord immunostaining or double IHC staining (GRP vs. SP).

Our double IHC using GRP and SP antibodies is consistent with studies in rats,[18] as well as supported by EM analysis revealing contacts not only between SP^{+} fibers but also GRP/SP fibers and GRPR neurons. Although SPergic fibers form contacts with GRPR neurons, it is unlikely for SP to communicate with GRPR neurons because they appear to lack NK1 receptor.[16] Interestingly, capsaicin treatment could induce SP, but not GRP, release from spinal cord slices.[57] Conversely, it is conceivable that GRP is selectively released from SP/

GRPergic fibers, but SP does not, in response to pruritogenic stimuli. It is also possible that SP in GRPergic fibers is selectively used to relay itch via NK1R neurons.[23]

Grp mRNA and GRP protein expression in the spinal cord

Of four recent independent investigations of the origin of GRP in the spinal cord using the dorsal rhizotomy, two studies, displaying both ipsilateral and contralateral side of the spinal cord in their entirety in one image, produced highly consistent results.[13,18] The other two, which argue for endogenous expression of GRP in the spinal cord, in fact were contradictory in respect to their GRP immunostaining in DRGs.[25,28] As aforementioned, a reasonable explanation for inconsistencies is likely due to the experimental protocols used rather than antibody specificity. More recently, we found that specific GRP immunostaining could be obtained using fresh DRG tissue without perfusion (data not shown). Notably, the finding that detection of *Grp* mRNA is refractory to ISH is reminiscent of the absence of *Npy* mRNA signal as examined by ISH in DRG.[58]

It has been known that not all mRNAs are translated into protein and a gene transcript could be translated into protein in one tissue but not the other. For example, although temporal and spatial expression pattern of *Grp* mRNA strikingly resembles that of GRP protein in lung tissue, some Grp^+ tissues were negative for GRP immunostaining.[59–63] Moreover, our unpublished data also indicate that in the brain, not all *Grp* mRNA-expressing areas are positive for GRP immunostaining. However, we are unable to exclude with certainty that GRP, upon translated by dorsal horn neurons, is rapidly degraded or GRP intrinsic to the dorsal horn falls below the threshold of IHC method we used. Such a possibility, however, is still compatible with the conclusion that a majority of GRPergic fibers in the spinal cord are of peripheral origin. Moreover, the present study further supports the notion the remaining GRP^+ fibers in the dorsal horn after the dorsal rhizotomy are perhaps of descending origin, because of the absence of GRP^+ immunostaining in dissociated dorsal horn neuronal culture.

Several studies have used the *Grp*-eGFP line which lack eGFP in DRGs as one of the evidence to argue that GRP protein is abundantly expressed in the dorsal horn but not in DRGs.[25,30,64] As we noted previously,[12] eGFP could be expressed even in knock-out mice with an eGFP knock-in. Conversely, eGFP in transgenic or knock-in mice may not be expressed in the regions where endogenous mRNA or protein of the gene of interest is present. While *Grp*-eGFP mice largely recapitulate endogenous *Grp* mRNA expression in the spinal cord, it is worth noting that expression of eGFP reporter protein only indicates *eGFP* mRNA transcription (thereby a surrogate for *Grp* mRNA), but the translation of the eGFP protein from *eGFP* mRNA cannot be used for an indication of the translation of GFP protein from *Grp* mRNA, because endogenous *Grp* mRNA, versus the eGFP mRNA, may be subject to distinct translational control.

Detection of Grp mRNA by RT-PCR, ISH, and RNA-seq

The present study indicates that the copy number of the *Grp* transcript is much lower than *Nmb*, *Tac1*, and *Mrgpra3* (Table 4). Thus, sufficient PCR cycles and incubation times for color development by ISH are also crucial for signal detection. Although both *Grp* and *Mrgpra3* are expressed in small percentage of DRGs, the level of *Grp* expression is approximately 90% lower than that of *Mrgpra3* according to RNA-Seq. This explains why it is easier to detect *Mrgpra3* than *Grp*. Although RNA-seq has been widely used for high-throughput profiling of gene expression, the technique could be limited by its inability to detect rare or low abundance of gene transcripts.[65,66] A key challenge is to increase the cell number rather than deeper sequencing.[67] For example, a single-cell RNA-seq has recently been applied to DRG neurons, revealing remarkable detailed transcriptome in a single-cell resolution. The study, however, failed to detect *Grp* mRNA based on average of 50 individual cells.[32] Given the low copy number of *Grp* transcripts expressed in very small percentage of DRGs, the reads for *Grp* mRNA could be zero or fall into the baseline noise if not enough cells are sampled. Other system errors which are inherently associated with RNA-seq may also skew the value for *Grp* mRNA.[68] To increase mRNA capture efficiency and overcome the limitation of single cells that can be sequenced, a droplet platform has been recently developed, enabling deep sequencing of a large number of cells instead of dozens or hundreds at a time.[69] In this regard, one may use *Grp* as a positive control to evaluate the sensitivity and coverage of the gene expression profiling with rare and low-copy number by RNA-seq.

The role of Grp mRNA vs. protein

The debate on the expression of GRP raises several interesting issues that are worth considering here. Concerning the specificity of the GRP antibody, a review of recent literature indicates that several groups were able to obtain specific GRP immunostaining in DRGs and their results are highly consistent (Table 1). Despite the demonstrated specificity of the GRP antibody, detection of distinct GRP immunostaining in subsets of DRGs remains challenging, as optimization of the immunostaining condition could be time-consuming. Some

researchers may be unwilling to spend weeks or even months on this. By contrast, it would be much easier to obtain widespread immunostaining using the GRP antibody if the condition is not optimized. Based on our own experience, detection of *Grp* positive signaling in DRGs by ISH is even more daunting, simply because of the low copies of *Grp* mRNA. This raises interesting questions that have puzzled some investigators. First, why is *Grp* mRNA expressed in the dorsal spinal cord if it is physiologically unimportant? One possibility is that spinal *Grp* may reflect an ontogenetic/evolutionary relic. Since the neural crest that gives rise to DRGs emerges from the dorsal neural tube,[70–72] many peptide genes in DRGs might have co-opted from the dorsal spinal cord and diverged to adopt novel functions, whereas their roles in the spinal cord became diminished. This enables the rapid and simple transduction of modality-specific information from the periphery to the spinal cord. Similarly, many postsynaptic receptors in the spinal cord crucial for relaying information encoded by primary afferents-released peptides may still reside in DRG, but they may have minimal functionality. Second, why is *Grp*/*Grpr* mRNA expression so low relative to some other genes if they are important itch genes? In DRGs, existing data do not suggest a positive correlation between abundance of a peptide and its physiological importance. For example, *Nppb* is more abundantly expressed than *Grp* in DRGs, but at least 10 times higher amount of BNP is required to evoke scratching behavior similar to that by GRP, even though the time course of the slow onset of scratching behavior does not support a direct activation of NPRA by BNP in the spinal cord.[12,17] From an evolutionary perspective, GRP may have been adopted to alert the body of pruritogenic stimuli. Given the relatively high affinity of GRP binding to its receptor, a transient and rapid release of GRP protein stored at the terminals of primary afferents should be sufficient to activate GRPR to evoke a few bouts of scratches, sub serving the warning mechanism. By contrast, a persistent and large amount of GRP release may trigger vicious scratch-itch cycles, resulting in a pathological itch condition.[13,40] As such, there is a need to minimize *Grp* mRNA in DRGs until GRP at the terminal is largely depleted. Similar to *Grp*, NPY peptide is present in the nerve terminals, but the level of its mRNA expression is very low in DRGs according to RNA-Seq, limiting its detection by ISH.[58] Thus, the level of *Grp* mRNA cannot be equated to that of GRP protein. One can envision that upon acute pruritogenic stimuli, GRP protein at the terminals could be rapidly released, while *Grp* mRNA translation may proceed slowly to maintain the level of GRP protein synthesis at a normal physiological state.

In summary, using a combination of molecular, anatomic, genetic, ISH, IHC, Western blot, RNA-seq, and ultrastructure analysis approaches, we demonstrate the presence of GRP in primary afferents as well as lack of evidence for GRP protein synthesis intrinsic to dorsal horn neurons. The present study indicates that the disagreement on GRP expression in DRGs and the antibody specificity is likely due to different IHC protocols used as well as low abundance of *Grp* mRNA in DRGs.

Acknowledgments

The authors thank the Genome Technology Access Center in the Department of Genetics at Washington University School of Medicine for help with genomic analysis. This publication is solely the responsibility of the authors and does not necessarily represent the official view of NCRR or NIH.

Author contributions

ZFC conceived the project and DMB, HL, YQL, and ZFC designed the experiments; DMB, HL, XYL, KFS, XTL, XJC, and JY performed experiments and data analysis. LH, ZYW, and YQL performed EM analysis; XJC and YGS conducted IHC independently, JY and AM contributed to the work and DMB, HL, XYL, YQL, and ZFC wrote the manuscript. DMB and HL contributed equally to this work.

Declaration of Conflicting Interests

The author(s) declared the following potential conflicts of interest with respect to the research, authorship, and/or publication of this article: The authors declare no competing financial interests.

Funding

The author(s) disclosed receipt of the following financial support for the research, authorship, and/or publication of this article: DMB was supported by W.M. Keck Fellowship and NIH-NIDA T32 Training Grant (5T32DA007261-23). Research reported in this publication was supported by AR056318-01A1 (Z.F.C), The National Natural Science Foundation of China (Grants 31371211 and 81371239) (HL and YQL). The National Natural Science Foundation of China (No. 31371122, 81322015), Chinese Academy of Sciences Hundreds of Talents Program (X.J.C and Y.G.S.). The Center is partially supported by NCI Cancer Center Support Grant #P30 CA91842 to the Siteman Cancer Center and by ICTS/CTSA Grant# UL1TR000448 from the National Center for Research Resources (NCRR), a component of the National Institutes of Health (NIH), and NIH Roadmap for Medical Research.

References

1. O'Donohue TL, Massari VJ, Pazoles CJ, et al. A role for bombesin in sensory processing in the spinal cord. *J Neurosci* 1984; 4: 2956–2962.
2. Massari VJ, Tizabi Y, Park CH, et al. Distribution and origin of bombesin, substance P and somatostatin in cat spinal cord. *Peptides* 1983; 4: 673–681.
3. Panula P, Hadjiconstantinou M, Yang HY, et al. Immunohistochemical localization of bombesin/gastrin-

releasing peptide and substance P in primary sensory neurons. *J Neurosci* 1983; 3: 2021–2029.
4. Panula P, Yang HY and Costa E. Neuronal location of the bombesin-like immunoreactivity in the central nervous system of the rat. *Regul Pept* 1982; 4: 275–283.
5. Decker MW, Towle AC, Bissette G, et al. Bombesin-like immunoreactivity in the central nervous system of capsaicin-treated rats: a radioimmunoassay and immunohistochemical study. *Brain Res* 1985; 342: 1–8.
6. Go VL and Yaksh TL. Quantification of bombesin-like peptides in mammalian spinal cord. *Ann N Y Acad Sci* 1988; 547: 70–75.
7. Kasprzyk PG, Cuttitta F, Treston AM, et al. Consideration of the chemistry of solid-phase matrix interaction leads to improved quantitation of neuropeptides. *Ann N Y Acad Sci* 1988; 547: 41–53.
8. Bautista DM, Wilson SR and Hoon MA. Why we scratch an itch: the molecules, cells and circuits of itch. *Nat Neurosci* 2014; 17: 175–182.
9. Jeffry J, Kim S and Chen ZF. Itch signaling in the nervous system. *Physiology (Bethesda)* 2011; 26: 286–292.
10. Geppetti P, Veldhuis NA, Lieu T, et al. G protein-coupled receptors: dynamic machines for signaling pain and itch. *Neuron* 2015; 88: 635–649.
11. Braz J, Solorzano C, Wang X, et al. Transmitting pain and itch messages: a contemporary view of the spinal cord circuits that generate gate control. *Neuron* 2014; 82: 522–536.
12. Liu XY, Wan L, Huo FQ, et al. B-type natriuretic peptide is neither itch-specific nor functions upstream of the GRP-GRPR signaling pathway. *Mol Pain* 2014; 10: 4.
13. Zhao ZQ, Huo FQ, Jeffry J, et al. Chronic itch development in sensory neurons requires BRAF signaling pathways. *J Clin Invest* 2013; 123: 4769–4780.
14. Zhao ZQ, Wan L, Liu XY, et al. Cross-inhibition of NMBR and GRPR signaling maintains normal histaminergic itch transmission. *J Neurosci* 2014; 34: 12402–12414.
15. Sun YG, Zhao ZQ, Meng XL, et al. Cellular basis of itch sensation. *Science* 2009; 325: 1531–1534.
16. Sun YG and Chen ZF. A gastrin-releasing peptide receptor mediates the itch sensation in the spinal cord. *Nature* 2007; 448: 700–703.
17. Kiguchi N, Sukhtankar DD, Ding H, et al. Spinal functions of B-type natriuretic peptide, gastrin-releasing peptide, and their cognate receptors for regulating itch in mice. *J Pharmacol Exp Ther* 2015; 356: 596–603.
18. Takanami K, Sakamoto H, Matsuda KI, et al. Distribution of gastrin-releasing peptide in the rat trigeminal and spinal somatosensory systems. *J Comp Neurol* 2014; 522: 1858–1873.
19. Liu Y, Abdel Samad O, Zhang L, et al. VGLUT2-dependent glutamate release from nociceptors is required to sense pain and suppress itch. *Neuron* 2010; 68: 543–556.
20. Lagerstrom MC, Rogoz K, Abrahamsen B, et al. VGLUT2-dependent sensory neurons in the TRPV1 population regulate pain and itch. *Neuron* 2010; 68: 529–542.
21. Nattkemper LA, Zhao ZQ, Nichols AJ, et al. Overexpression of the gastrin-releasing peptide in cutaneous nerve fibers and its receptor in the spinal cord in primates with chronic itch. *J Invest Dermatol* 2013; 133: 2489–2492.
22. Tominaga M, Ogawa H and Takamori K. Histological characterization of cutaneous nerve fibers containing gastrin-releasing peptide in NC/Nga mice: an atopic dermatitis model. *J Invest Dermatol* 2009; 129: 2901–2905.
23. Akiyama T, Tominaga M, Takamori K, et al. Roles of glutamate, substance P, and gastrin-releasing peptide as spinal neurotransmitters of histaminergic and nonhistaminergic itch. *Pain* 2014; 155: 80–92.
24. Satoh K, Takanami K, Murata K, et al. Effective synaptome analysis of itch-mediating neurons in the spinal cord: a novel immunohistochemical methodology using high-voltage electron microscopy. *Neurosci Lett* 2015; 599: 86–91.
25. Solorzano C, Villafuerte D, Meda K, et al. Primary afferent and spinal cord expression of gastrin-releasing peptide: message, protein, and antibody concerns. *J Neurosci* 2015; 35: 648–657.
26. Liu T, Berta T, Xu ZZ, et al. TLR3 deficiency impairs spinal cord synaptic transmission, central sensitization, and pruritus in mice. *J Clin Invest* 2012; 122: 2195–2207.
27. Alemi F, Kwon E, Poole DP, et al. The TGR5 receptor mediates bile acid-induced itch and analgesia. *J Clin Invest* 2013; 123: 1513–1530.
28. Fleming MS, Ramos D, Han SB, et al. The majority of dorsal spinal cord gastrin releasing peptide is synthesized locally whereas neuromedin B is highly expressed in pain- and itch-sensing somatosensory neurons. *Mol Pain* 2012; 8: 52.
29. Liu Q, Tang Z, Surdenikova L, et al. Sensory neuron-specific GPCR Mrgprs are itch receptors mediating chloroquine-induced pruritus. *Cell* 2009; 139: 1353–1365.
30. Mishra SK and Hoon MA. The cells and circuitry for itch responses in mice. *Science* 2013; 340: 968–971.
31. Wada E, Way J, Lebacq-Verheyden AM, et al. Neuromedin B and gastrin-releasing peptide mRNAs are differentially distributed in the rat nervous system. *J Neurosci* 1990; 10: 2917–2930.
32. Usoskin D, Furlan A, Islam S, et al. Unbiased classification of sensory neuron types by large-scale single-cell RNA sequencing. *Nat Neurosci* 2015; 18: 145–153.
33. Goswami SC, Thierry-Mieg D, Thierry-Mieg J, et al. Itch-associated peptides: RNA-Seq and bioinformatic analysis of natriuretic precursor peptide B and gastrin releasing peptide in dorsal root and trigeminal ganglia, and the spinal cord. *Mol Pain* 2014; 10: 44.
34. Xiao HS, Huang QH, Zhang FX, et al. Identification of gene expression profile of dorsal root ganglion in the rat peripheral axotomy model of neuropathic pain. *Proc Natl Acad Sci USA* 2002; 99: 8360–8365.
35. Cao YQ, Mantyh PW, Carlson EJ, et al. Primary afferent tachykinins are required to experience moderate to intense pain. *Nature* 1998; 392: 390–394.
36. Jeffry JA, Yu SQ, Sikand P, et al. Selective targeting of TRPV1 expressing sensory nerve terminals in the spinal cord for long lasting analgesia. *PLoS One* 2009; 4: e7021.
37. Akiyama T, Carstens MI and Carstens E. Enhanced scratching evoked by PAR-2 agonist and 5-HT but not histamine in a mouse model of chronic dry skin itch. *Pain* 2010; 151: 378–383.

38. Miyamoto T, Nojima H, Shinkado T, et al. Itch-associated response induced by experimental dry skin in mice. *Jpn J Pharmacol* 2002; 88: 285–292.
39. Liu XY, Liu ZC, Sun YG, et al. Unidirectional cross-activation of GRPR by MOR1D uncouples itch and analgesia induced by opioids. *Cell* 2011; 147: 447–458.
40. Zhao ZQ, Liu XY, Jeffry J, et al. Descending control of itch transmission by the serotonergic system via 5-HT1A-facilitated GRP-GRPR signaling. *Neuron* 2014; 84: 821–834.
41. Chen ZF, Rebelo S, White F, et al. The paired homeodomain protein DRG11 is required for the projection of cutaneous sensory afferent fibers to the dorsal spinal cord. *Neuron* 2001; 31: 59–73.
42. Dobin A, Davis CA, Schlesinger F, et al. STAR: ultrafast universal RNA-seq aligner. *Bioinformatics* 2013; 29: 15–21.
43. Jensen RT, Battey JF, Spindel ER, et al. International union of pharmacology. LXVIII Mammalian bombesin receptors: nomenclature, distribution, pharmacology, signaling, and functions in normal and disease states. *Pharmacol Rev* 2008; 60: 1–42.
44. Panula P, Nieminen O, Falkenberg M, et al. Localization and development of bombesin/GRP-like immunoreactivity in the rat central nervous system. *Ann N Y Acad Sci* 1988; 547: 54–69.
45. Yoshida A, Chen K, Moritani M, et al. Organization of the descending projections from the parabrachial nucleus to the trigeminal sensory nuclear complex and spinal dorsal horn in the rat. *J Comp Neurol* 1997; 383: 94–111.
46. Steinhoff MS, von Mentzer B, Geppetti P, et al. Tachykinins and their receptors: contributions to physiological control and the mechanisms of disease. *Physiol Rev* 2014; 94: 265–301.
47. Bardoni R, Tawfik VL, Wang D, et al. Delta opioid receptors presynaptically regulate cutaneous mechanosensory neuron input to the spinal cord dorsal horn. *Neuron* 2014; 81: 1312–1327.
48. Guan JS, Xu ZZ, Gao H, et al. Interaction with vesicle luminal protachykinin regulates surface expression of delta-opioid receptors and opioid analgesia. *Cell* 2005; 122: 619–631.
49. Sims D, Sudbery I, Ilott NE, et al. Sequencing depth and coverage: key considerations in genomic analyses. *Nat Rev Genet* 2014; 15: 121–132.
50. Carstens EE, Carstens MI, Simons CT, et al. Dorsal horn neurons expressing NK-1 receptors mediate scratching in rats. *Neuroreport* 2010; 21: 303–308.
51. Pavlovic S, Daniltchenko M, Tobin DJ, et al. Further exploring the brain-skin connection: stress worsens dermatitis via substance P-dependent neurogenic inflammation in mice. *J Invest Dermatol* 2008; 128: 434–446.
52. Ohmura T, Tsunenari I, Hayashi T, et al. Role of substance P in an NC/Nga mouse model of atopic dermatitis-like disease. *Int Arch Allergy Immunol* 2004; 133: 389–397.
53. Tobin D, Nabarro G, Baart de la Faille H, et al. Increased number of immunoreactive nerve fibers in atopic dermatitis. *J Allergy Clin Immunol* 1992; 90: 613–622.
54. Fantini F, Pincelli C, Romualdi P, et al. Substance P levels are decreased in lesional skin of atopic dermatitis. *Exp Dermatol* 1992; 1: 127–128.
55. Grip L, Lonne-Rahm SB, Holst M, et al. Substance P alterations in skin and brain of chronically stressed atopic-like mice. *J Eur Acad Dermatol Venereol* 2013; 27: 199–205.
56. Saper CB. A guide to the perplexed on the specificity of antibodies. *J Histochem Cytochem* 2009; 57: 1–5.
57. Moody TW, Pert CB, Rivier J, et al. Bomebesin: specific binding to rat brain membranes. *Proc Natl Acad Sci USA* 1978; 75: 5372–5376.
58. Ji RR, Zhang X, Wiesenfeld-Hallin Z, et al. Expression of neuropeptide Y and neuropeptide Y (Y1) receptor mRNA in rat spinal cord and dorsal root ganglia following peripheral tissue inflammation. *J Neurosci* 1994; 14: 6423–6434.
59. Sunday ME. Tissue-specific expression of the mammalian bombesin gene. *Ann NY Acad Sci* 1988; 547: 95–113.
60. Spindel ER, Sunday ME, Hofler H, et al. Transient elevation of messenger RNA encoding gastrin-releasing peptide, a putative pulmonary growth factor in human fetal lung. *J Clin Invest* 1987; 80: 1172–1179.
61. Sunday ME, Wolfe HJ, Roos BA, et al. Gastrin-releasing peptide gene expression in developing, hyperplastic, and neoplastic human thyroid C-cells. *Endocrinology* 1988; 122: 1551–1558.
62. Li K, Nagalla SR and Spindel ER. A rhesus monkey model to characterize the role of gastrin-releasing peptide (GRP) in lung development. Evidence for stimulation of airway growth. *J Clin Invest* 1994; 94: 1605–1615.
63. Wang D, Yeger H and Cutz E. Expression of gastrin-releasing peptide receptor gene in developing lung. *Am J Respir Cell Mol Biol* 1996; 14: 409–416.
64. Gutierrez-Mecinas M, Watanabe M and Todd AJ. Expression of gastrin-releasing peptide by excitatory interneurons in the mouse superficial dorsal horn. *Mol Pain* 2014; 10: 79.
65. Clark MB, Mercer TR, Bussotti G, et al. Quantitative gene profiling of long noncoding RNAs with targeted RNA sequencing. *Nat Methods* 2015; 12: 339–342.
66. Jiang L, Schlesinger F, Davis CA, et al. Synthetic spike-in standards for RNA-seq experiments. *Genome Res* 2011; 21: 1543–1551.
67. Kolodziejczyk AA, Kim JK, Svensson V, et al. The technology and biology of single-cell RNA sequencing. *Mol Cell* 2015; 58: 610–620.
68. Wang Z, Gerstein M and Snyder M. RNA-Seq: a revolutionary tool for transcriptomics. *Nat Rev Genet* 2009; 10: 57–63.
69. Klein AM, Mazutis L, Akartuna I, et al. Droplet barcoding for single-cell transcriptomics applied to embryonic stem cells. *Cell* 2015; 161: 1187–1201.
70. Ding YQ, Yin J, Kania A, et al. Lmx1b controls the differentiation and migration of the superficial dorsal horn neurons of the spinal cord. *Development* 2004; 131: 3693–3703.
71. Le Douarin NM and Smith J. Development of the peripheral nervous system from the neural crest. *Annu Rev Cell Biol* 1988; 4: 375–404.
72. Green SA, Simoes-Costa M and Bronner ME. Evolution of vertebrates as viewed from the crest. *Nature* 2015; 520: 474–482.